MAE 4353
Mechanical Design II
Spring 2025

PROJECT TITLE:

DESIGN AND ANALYSIS OF REFINERY STACK SUPPORT BEAMS WITH WELDED AND BOLTED CONNECTIONS

Project Manager: Student Class #: Grade: .

Research Lead: Student Class #: Grade: .

Design Lead: Student Class #: Grade: .

Validation Lead: Student Class #: Grade: .

Evaluation Lead: Jordan Pascoe Class #: Grade: .

Total Grade:____________

PROJECT (30%):

Project report will be a group assignment. It is required that every student in the group participates in writing the report. It is an opportunity for every student to different skill sets. The team will consist of: Each one of you will submit the final document in your respective canvas assignment sheet.

Project Manager:	Manage the RDT&E team by assign tasks, monitor progress, approve outcomes or reassign tasks if the work quality is inadequate. Prepare the cover page with the name and task of each member. Write the executive summary (abstract) and the (conclusion) section and submit the final report.
Research Lead:	Explore and Hypothesize. Conduct the literature review, compile a list of references and write the (Introduction, literature review, and specific objectives).
Design Lead:	Design calculations and analysis, Make a sketch of the design, write the section.
Validation Lead:	Testing the design and validation. Generate and (tabulate) the solutions, report the flaws, etc. Produce all needed calculations.
Evaluation Lead:	Synthesize and Theorize. Plot all (graphs), analyze the results to write the (Results & Discussion) section.

Summary of Contributions

Student 1: Student

- Initial CAD drawings
- Load Analysis
- Bolt Calculations
- Optimization

Student 2: Student

- Introduction
- References
- Report formatting
- Assisting in other sections

Student 3: Student

- Design philosophy
- Fatigue theory analysis
- Conclusion

Student 4: Student

- CAD drawings
- FMEA
- Case Studies
- Weld Calculations

Student 5: Jordan Pascoe

- Risk Analysis
- Oscillation Calculations

Table of Contents

Introduction 6
Literature Review 7
Design Philosophy 9
Risk Analysis 10
Case Studies 12
Case 1: Ideal Conditions 12
Case 2: Worst Conditions 13
Design Calculations 14
Load Analysis 14
Case 1: Ideal Conditions, Beam-1 Analysis 14
Case 1: Ideal Conditions, Beam-2 Analysis 19
Case 2: Worst-Case Scenario 22
Bolt Calculations 25
Welding Calculations 31
Oscillation Analysis 33
Optimization 41
Failure Theory and Fatigue Analysis 43
CAD Drawings 45
FMEA 50
FEA Analysis 51
Case 1: Ideal Conditions 52
Case 2: Worst Conditions 53
.... 53
Conclusion 55
References 56
Appendix 57
Oscillation Python Code 57

Table of Figures:

Figure 1: Case Study 1 Top View 19
Figure 2: Case Study 2 Side View 19
Figure 3: Case Study 2 Top View 20
Figure 4: Case Study 2 Side View 20
Figure 5: Loading Diagram 21
Figure 6: Shear Diagram 21
Figure 7: Moment Diagram 22
Figure 8: Deflection Diagram 22
Figure 9: Appendix A-9, Fixed Supports 23
Figure 10: Appendix A-9, Fixed Supports 23
Figure 11: Loading Diagram 28
Figure 12: Shear Diagram 28
Figure 13: Moment Diagram 28
Figure 14: Deflection Diagram 29
Figure 15: Loading Diagram 31
Figure 16: Shear Diagram 31
Figure 17: Moment Diagram 32
Figure 18: Deflection Diagram 32
Figure 19: Side View Bolt Assembly 34
Figure 20: Isometric View of Bolt Assembly 34
Figure 21: Hardware Design 34
Figure 22: Free Body Diagram of Beam 36
Figure 23: Shear Load Resultant Diagram 37
Figure 24: Wind Velocity streamlines from North to South 43
Figure 25: Drag Coefficient 46
Figure 26: Free-Body Diagram 47
Figure 27: Velocity streamlines going West to East 48
Figure 28: Flow from Laminar to Turbulent 48
Figure 29: Oscillations of Refinery Stack 49
Figure 30: Results from Python Code Velocity streamlines at 120 degrees 50
Figure 31: Right side view of refinery stack 55
Figure 32: Left side view of refinery stack 55
Figure 33: Top view of refinery stack 56
Figure 34: Top view of Overall Refinery stack with support system design 56
Figure 35: Bottom view overall support system 57
Figure 36: Side View of overall support system 57
Figure 37: Bottom View Slotted Bolts and with Collar 58
Figure 38: Side View Bolts positioning 58
Figure 39: Bottom view of the Beam with support 59
Figure 40: FMEA 60
Figure 41: Ideal Conditions FEA 62
Figure 42: Worst Case FEA 63
Figure 43: Calculated vs FEA comparison 64

Table of Tables:

Table 1: Risk Analysis Matrix....16
Table 2: Mitigation Strategies....17
Table 3: Resulting Load Conditions on Beam-1....22
Table 4: Beam-1 Reaction Forces....23
Table 5: Beam-1 Shear Forces....24
Table 6: Beam-1 Moments....25
Table 7: Beam-1 Deflection....26
Table 8: Beam-1 Online Beam Calculator vs Hand Calculations....26
Table 9: Resulting Load Conditions on Beam-2....29
Table 10: Beam-2 Tabulated Hand Calculation Results....30
Table 11: Beam-2 Online Beam Calculator vs Hand Calculations....30
Table 12: Online Calculator Results....32
Table 13: Tabulated Hand Calculation Results....33
Table 14: Beam-2 Online Beam Calculator vs Hand Calculations....33
Table 15: Requirements to Secure Bolt....35
Table 16: Shear Load Analysis....37
Table 17: Bearing Stress....38
Table 18: Critical Bending Stress Results....39
Table 19: Initial Conditions....43
Table 20: Constants....44
Table 21: Material Properties and Dimensions....45
Table 22: Structural Area and Volume Calculations....45
Table 23: Oscillation Calculation Results....47
Table 24: Analytical results comparing beam configurations based on structural performance and cost efficiency....51
Table 25: Bolt optimization based on shear stress and safety factors across varying diameters....52
Table 26: Deflection Comparison....63

Table of Equations:

Equation 1: Reaction 1 23
Equation 2: Reaction 2 23
Equation 3: Reactions 23
Equation 4: Shear Force AB 24
Equation 5: Shear Force BC 24
Equation 6: Shear Force 24
Equation 7: Moment 1 24
Equation 8: Moment 2 24
Equation 9: Moments 24
Equation 10: Deflection 1 26
Equation 11: Deflection 2 26
Equation 12: Maximum Deflection 26
Equation 13: Torque 35
Equation 14: Pre-loading Force 35
Equation 15: Shearing Load per Bolt 36
Equation 16: Secondary Shearing Load per Bolt 36
Equation 17: Area of Circle 38
Equation 18: Shear Stress 38
Equation 19: Factor of Safety 38
Equation 20: Bearing Area 38
Equation 21: Bearing Stress 38
Equation 22: Bending Stress 39
Equation 23: Moment 39
Equation 24: Weld Size 40
Equation 25: Stress 40
Equation 26: Throat Area 40
Equation 27: Newton’s Second Law 44
Equation 28: Moment 44
Equation 29: Drag Force 44
Equation 30: Amplitude 44
Equation 31: Natural Frequency 44
Equation 32: Damped Natural Frequency 44
Equation 33: Damping Ratio 44
Equation 34: Differential Equation of Motion 44
Equation 35: Harmonic Equation for Displacement 44
Equation 36: Reynold’s Number 44
Equation 37: Drag Coefficient 44
Equation 38: Dynamic Pressure 44
Equation 39: Stiffness 44
Equation 40: Stress 53
Equation 41: Bending Stress 53
Equation 42: Maximum Deflection 53
Equation 43: Goodman Fatigue 53
Equation 44: Shear Stress 54
Equation 45 Factor of Safety 54

Introduction

Refinery stacks are critical structures in petroleum processing facilities, serving as exhaust outlets that safely release gases produced during refining operations. These towering cylindrical stacks must remain structurally stable while enduring various external forces, including wind loads, cyclic stresses, and oscillatory movement. Given their exposure to these dynamic environmental conditions, refinery stacks often require interconnecting support beams to maintain alignment, distribute loads, and mitigate excessive movement. Without proper reinforcement, repeated oscillations and environmental stresses could lead to misalignment, fatigue failure, or structural instability over time.

The objective of this design project is to develop a structurally sound and adaptable beam system that effectively links two refinery stacks while accommodating predefined constraints and operational demands. The proposed design consists of two offset I-beams connecting the stacks, providing enhanced stability and load-bearing capacity. These beams will be secured using partial collars, brackets, and bolted connections, ensuring a strong yet flexible attachment. The design must account for periodic oscillations of the stacks while preventing excessive stress concentrations at the connection points. This design ensures that the beam system remains structurally sound while preventing excessive stress concentrations on the stacks.

The design must meet strict geometric, structural, and environmental constraints to ensure its feasibility in an industrial setting. These conditions include:

- Stack Movement: Each stack undergoes 2.625 inches of oscillation every 13 minutes, requiring the beam system to accommodate this periodic motion without excessive fatigue or structural damage.
- Load Requirements: The beam must support an industry-standard live load of 75 psf, ensuring adequate strength for operational conditions.
- Wind Load: At the platform location, the beam must withstand a wind force of 1,615 lbf, necessitating proper load distribution and robust anchoring.
- Stack Shell Thickness: The stacks have a 5/16-inch thick shell, imposing constraints on connection design to prevent localized stress concentrations that could weaken the structure over time.
- Beam Dimensions: The beam height is constrained between 6 and 12 inches, with a width limitation of 6 to 8 inches and a length of 97.5 inches. These limitations will influence the selection of materials and the beam's cross-sectional profile.
- Material Selection: The chosen material must provide high strength, durability, and corrosion resistance, ensuring long-term performance in the harsh refinery environment.

To ensure compliance with these constraints, two offset I-beams will be used instead of a single beam, a design choice that enhances load distribution and redundancy. This approach provides greater resistance to bending and torsional forces while maintaining flexibility under dynamic loading conditions. A partial collar connection, which wraps partially around the stacks to evenly distribute forces and minimizes localized stress concentrations, will secure the beams to the stacks.

Additionally, brackets and bolted connections will be implemented to improve stability, ease of installation, and future maintenance accessibility.

This report will provide an in-depth analysis of the beam system's design, beginning with an explanation of the design philosophy, including the rationale behind the use of offset I-beams, partial collars, brackets, and bolted connections. A risk analysis will be conducted to identify potential failure mechanisms, including fatigue, stress concentrations, and excessive deformation due to cyclic loading. Case studies of similar structural applications will be reviewed to support design decisions and incorporate best practices in the industry.

A detailed mechanical analysis will be performed, covering stress distributions, deformation calculations, moment and force evaluations, and safety factor determinations. Given the recurring oscillations experienced by the structure, fatigue theory will be a critical aspect of the analysis to ensure long-term durability. The report will also include CAD drawings and properly dimensioned technical sketches to illustrate the final design clearly. Additionally, SolidWorks analysis will be utilized to further validate the beam system's performance, providing insight into stress distribution, deformation characteristics, and potential failure points.

By integrating analytical and computational approaches, this project aims to deliver a refined, structurally efficient, and industry-compliant support beam system that enhances the stability and longevity of refinery stacks. Through careful design considerations, material selection, and connection optimization, this system will provide a robust solution tailored to the demands of an operational refinery environment.

Literature Review

In industrial systems where flare stacks are supported by external beams, the design of those beams and their connections must account for complex loading conditions imposed by the stacks. Since the stacks themselves are fixed in geometry and material—5/16-inch thick 836 steel—support structures must compensate for any dynamic and thermal stresses transmitted through the connection interface. Literature on structural behavior in such environments highlights the importance of robust beam design, fatigue resistance, and compliant connections to manage induced oscillations and heat transfer from flare operations.

Dynamic loads originating from stack oscillations, whether caused by combustion variability or environmental factors like wind, can propagate into the supporting beams. While flare stacks are typically designed to reduce self-excited resonance, the support beams must still accommodate any transmitted motion, especially under "ideal" conditions where resonance is more easily sustained (Seshadri, Buell, & Mehta, 2005). Beams must therefore be evaluated using high-cycle fatigue analysis, accounting for fluctuating stress inputs even if vibration amplitudes remain small. Tools such as the Goodman or Gerber criteria are particularly useful for evaluating fatigue limits under combined mean and alternating stresses, especially when connections are subject to stress concentrations.

Thermal exposure is another major factor influencing beam design. Although the primary heat source is localized to the flare tip, radiated and conducted heat through the connection area can introduce thermal gradients within the beam structure. NIST research on I-beams subjected to non-uniform heat exposure showed that localized heating—combined with restraint or fixed-end conditions—can shift failure locations to the points of highest mechanical stress, not necessarily the hottest regions (NIST, 2005). For the support beam, this implies that even moderate thermal gradients could increase vulnerability if combined with high connection stiffness or restrained thermal expansion. Therefore, it is important to allow for controlled flexibility in the beam's connection design—such as through slotted connections or expansion-compatible interfaces—to reduce thermal stress buildup.

ASME STS-1 design guidelines further emphasize the importance of integrating thermal and dynamic considerations into structural support elements, even when stack geometry is fixed (ASME, 2000). The inclusion of vibration-dampening systems within the beam structure, or near the connection points, can reduce the transmission of dynamic loads and enhance fatigue life. While such systems are more commonly applied at the stack level, similar concepts may be adapted for support beams—particularly if the beam is segmented for transportation and must accommodate multiple bolted or welded joints. Bolted joints should be analyzed for preload, fatigue life, and joint separation risk, while welded joints must be evaluated for combined shear and bending fatigue using conservative stress models.

In summary, while the flare stack design is fixed, the support beam and its joints must be carefully engineered to accommodate the dynamic and thermal loads that originate from stack operation. Fatigue analysis, thermal flexibility, and ASME-aligned connection detailing are critical to ensuring long-term structural integrity under fluctuating conditions.

Design Philosophy

The objective of this design is to develop a structurally sound support beam system that connects a pair of refinery stacks and safely resists all operational and environmental loads. The design must account for static and dynamic forces, thermal effects, and potential oscillatory behavior caused by stack movement and wind. A key constraint is the fixed span between stacks, with allowable beam cross-sectional dimensions limited to a height between 6 and 12 inches and a width between 6 and 8 inches. These limitations required careful material selection and stress optimization to ensure strength without overdesign.

Over weeks of concept development and analysis, multiple configurations were explored, including variations in beam shapes, connection methods, and material choices. These iterative discussions allowed the design team to evaluate feasibility, requirements, and simplicity. The final design reflects a synthesis of these evaluations, aiming to provide both performance and practicality. To meet these requirements, the beam was designed using a dual-member configuration to facilitate transportation, reduce fabrication complexity, and provide potential redundancy. The beam is connected to the stacks using both bolts and welds—bolted joints provide ease of disassembly and field adjustability, while fillet welds offer permanent structural support and help distribute load smoothly. The welds were sized based on allowable shear stress calculations and verified against yield strength using a conservative safety factor of 3.

Design decisions were guided by mechanical design principles outlined in Shigley's Mechanical Engineering Design and aligned with ASME code recommendations for industrial structures. All structural components were analyzed for axial, shear, and bending stresses, and failure theories—including fatigue and safety factor evaluations—were applied to critical joints. The expected stack movement of 2.625 inches and wind load of 1,615 lbf at platform level were key considerations in load simulation and material strength validation.

The overall design balances durability, ease of assembly, code compliance, and long-term reliability, ensuring that the support structure performs effectively under cyclic loading and extreme conditions typical of flare stack environments.

Our reasoning behind why we designed our system to have two support beams is based on several critical factors.

First, the decision to implement two beams instead of a single larger beam was driven by the need to enhance load distribution and improve system redundancy. With two beams, the load generated by wind forces, live loads, and oscillatory movement is shared more evenly between the two members. This reduces peak stress concentrations within each beam and at the connection points, therefore increasing the fatigue life of the system.

Second, transportation and handling constraints played a major role. A single, larger beam that meets the required strength and deflection criteria would have been significantly heavier and more cumbersome to fabricate, transport, and install. By splitting the system into two smaller, standard-sized beams, we simplified logistics, reduced installation complexity, and minimized field adjustments—a major advantage in refinery environments where crane and lift capacities are often limited.

Third, the dual-beam configuration improves flexibility in accommodating thermal expansion and stack oscillation. Each beam is independently connected with bolted and welded joints, and the use of spacers and slotted bolt holes further allows for controlled movement without over-constraining the system. This design prevents excessive internal stresses during daily thermal cycles and wind-induced stack swaying, which could otherwise lead to cracking or fatigue failures.

In terms of weight considerations, while adding a second beam does increase the total mass of the system slightly, the design is optimized so that the individual beams remain within the allowable geometric constraints (6–12 inches height, 6–8 inches width) and are not oversized. The added weight is minimal compared to the substantial benefits in redundancy, durability, and ease of maintenance. Additionally, the load calculations and risk analysis confirmed that the supporting structures can handle the combined weight without introducing additional structural risks.

Each major component was carefully chosen to complement this design philosophy:

- Offset I-beams: Maximized moment of inertia for bending resistance within dimensional constraints.
- Partial collars: Distributed attachment forces over a larger area of the stack shell to avoid stress concentrations.
- Slotted bolt connections: Allowed for necessary movement due to oscillations and thermal expansion while maintaining secure fastening.
- Spacers in bolt assemblies: Prevented clamping-induced distortions and permitted a more flexible, slip-resistant connection.
- Fillet welds: Sized conservatively to handle shear forces safely, enhancing joint reliability without over-welding and inducing unwanted thermal stresses.

Ultimately, the two-beam system offers superior performance, safety, and longevity compared to a single beam solution. It is a deliberate choice reflecting engineering best practices for dynamic, high-risk environments like refinery stack structures.

Risk Analysis

An imperative portion of the design process of the support and reinforcement system for the refinery stack is the risk analysis. In totality, the risk analysis entails many imperative considerations that will govern the design process and will dictate finding the equilibrium between sustainability and optimization. The key aspect of the risk analysis is to determine and identify potential areas of failure and conduct an assessment in evaluating the impact of the failures, the severity, the probability of the occurrence of the failure. The process involves the structural integrity of the refinery stack, material properties, environmental conditions, location and terrain characteristics, beam design and loading considerations. By methodically and maliciously evaluating the risk and potential hazards a mitigation plan can be formulated.

Firstly, the environmental conditions, location and terrain characteristics will be major determinant in understanding and evaluating how to design the support system for the refinery stack. Assuming the refinery stack will be locally based within Tulsa County or surrounding counties, the refinery stack will be subjected to severe wind conditions, drastic intraday temperature differential, and for more extreme conditions such as tornadoes, and earthquakes will create a marginal complexity layer to the analysis. Wind speeds in Tulsa County can range but it is frequent enough to consider wind speeds greater than thirty miles per hour. At those great wind speeds, it will induce adequately sized wind loads which will create oscillations and vibrations within the system which corresponds to cyclical relationship of compressive and tensile forces. Over time, the cyclical relationship may cause fatigue and material failure. The temperature gradient intra-day and seasonally varying temperature ranges, the support system components will be affected by thermal expansions which can lead to deformation and structural elongation. Dependent upon the use of rigid connections and flexibility of the design it can create significant stresses that can lead to structural fatigue or cracking.

The risks of structural integrity can be jeopardized from one or a combination of different types of loading, material selection, types of connections such as bolting techniques and torque specifications and welding. The refinery stack will experience variety of factors, one be of such live loading entailing equipment and personal, if the limitation of the live loading conditions is exceeded it can lead to structural blemishes such as cracking and dependent upon the frequency; permanent deformation or breakage. The wind load will cause oscillation, and if the rigidity of the refinery stack is sufficient it will increase the drag which will induce excessive vibrations. The vibrations can cause connection components to become loose and contribute to the cyclic stresses, and instability of components. The selection of materials and their corresponding properties will heavily influence the structural integrity due to the unique properties. The materials being selected should include the atomic structure, the stiffness, strength, hardness, ductility, and toughness in conjunction to how the material were created or treated. It would be idealistic to find materials that would be adequate in all those values when designing the support structure. Also, the material will experience corrosion or degradation over time due to moisture, temperature, chemicals.

With identification of potential risks and hazards, possible solutions can be derived, and optimization can be taken into account. Based upon the wind loading conditions one solution is to make the refinery stack bracing less rigid and flexible to aid in the mitigation of drag forces and excessive vibrations. The components can be external treated to it may have longevity in the prevention of degradation. With dynamic loading scenarios, it will entail eccentric loading and adding the proper reinforcement to offset the load. To placate the amplitude of the oscillation it is having tension cables, or a damper could be implemented. In totality, the identification of risks will promote solution methods in negating the potential hazards and risks. The below is a risk analysis matrix to properly convey frequency of risks occurring and severity. The risk analysis matrix is has severity that goes from negligible to catastrophic which is minimal to maximal impact. The frequency of occurrences goes from very probable to rare, it translate to common to rare. The color coded system is defined as minimal intervention and maintenance to maximal intervention and maintenance.

	Very Probable	**Probable**	**Potential**	**Improbable**	**Very Improba ble**	**Rare**
Negligible	Ultraviolet Fading of Paint Coating	Non-Critical Surface Rust	Aesthetic Misalignment	Paint Bubbling	Minor Galvanic Reaction	Bolt Head Abrasion
Minor	Excessive Deflection Causing Misalignment	Uneven Bolt Tension	Inconsistent Weld Penetration	Bracket Fatigue Crack Initiation		
Moderate	Exposure Bare Metal	Weld Spatter Stress Risers	Vibration-Induced Bolt Loosening	Flange Bending		
Significant	Corroded Welds	Beam Misalignmen t	Oversized Weld causing Thermal Warping	Spacer Deformation	Creep in Bolted Joint	
Severe	Thermal Expansion Cracking	Long Term Fatigue From Wind	Loose Bolts Causing Joint Slip	Spacer Crushing Under Eccentric Loading	Buckling Under Misapplie d Live Load	
Catastrophic	Beam Weld Rupture During Oscillation	Seismic Induced Collapse	Combined Bolt and Weld Failure under Wind Loading			

Table 1: Risk Analysis Matrix

The defining failure types listed and graded in Table 1 are tailored to the refinery stack being built in Tulsa, Oklahoma region. The wind loading and potential earthquakes can have catastrophic failure to complete destruction of the refinery stack. Also, due to excessive sun exposure there will be cosmetic decay that will be need to be addressed over time. Table 2 is the mitigation strategies, it goes over the types of failure presented in Table 1 and presents potential solutions to mitigate the type of failure from worsening or altogether prevent is from occurring.

Type of Failure	Mitigation
Bolt Head Abrasion	Protective Caps
Minor Galvanic Reaction	Use of washers to maintain separation
Paint Bubbling	Prepare surface and apply new coating of paint
Aesthetic Asymmetry	Offset
Surface Rust	Grind surface and apply primer
Ultraviolet Fading of Paint	Apply UV resistant paint
Bracket Fatigue Crack Initiation	Use Radi cutouts, notches or fillets
Inconsistent Weld Penetration	Inspect weld quality
Uneven Bolt Tension	Apply appropriate torque specifications
Excessive Deflection Causing Misalignment	Calculate Stiffness
Flange Bending	Reinforce Flanges or redistribute loads
Vibration Induced Bolt Loosening	Use locking washers
Weld Spatter Stress Risers	Post weld cleanup
Bare Metal Exposure	Use UV and weather resistance paint
Creep in Bolted Joint	Use bolts heat treated, torque to an appropriate specification
Spacer Deformation	Use hardened steel or alloys spacers
Oversized Weld causing Thermal Warping	Preheat or cool welded areas
Buckling Under Misapplied Live Load	Use stiffeners, buckling analysis
Spacer Crushing Under Eccentric Loading	Use hardened spacers, increase the surface area of the spacer
Beam Misalignment	Alignment components
Corroded Welds	Apply zinc coatings
Loose Bolts Causing Slip Joints	Use locking nuts, double nuts, thread-locking compound
Long-Term Fatigue From Wind	Use S-N curve, add dampers
Thermal Expansion Cracking	Include slotted bolt holes, flexible joints, materials with adequate temperature properties
Combined Bolt and Weld Failure Under Wind Loading	Include redundant fasteners or dual loading paths
Seismic Induced Collapse	Add lateral braces and/ or flexible joints
Beam Weld Rupture During Oscillation	Use high strength fillet welds and simulate dynamic loading

Table 2: Mitigation Strategies

Case Studies

Case 1: Ideal Conditions

Background: Flare stacks and surrounding structures have many connections to be considered. Especially considering the necessity of reliable support of flaring systems.

Scenario: The beam is being analyzed on an average day in Tulsa, Oklahoma, where the winds are negligible, and the ambient temperature is 90°F. There is no heavy flaring, so the beams generally are at ambient temperatures. Movement of the stacks is negligible. The live load is 75psf, including a 357lb load roughly 4ft from the center of the left flare center, and a 234lb load roughly 4.5ft from the right flare center. The flare stack shell thickness is 5/16 inches. There are no significant oscillations in the flare stack and surrounding structure. There is no seismic activity on this calm day in Tulsa. The only forces are in the x direction due to gravity.

Findings: The beam is designed to meet safe criteria and does not exhibit any extreme fluctuation or movement.

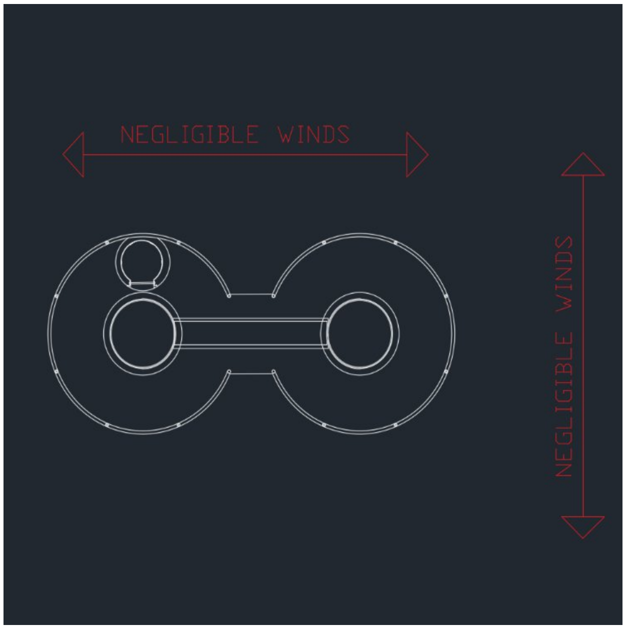

Figure 1: Case Study 1 Top View

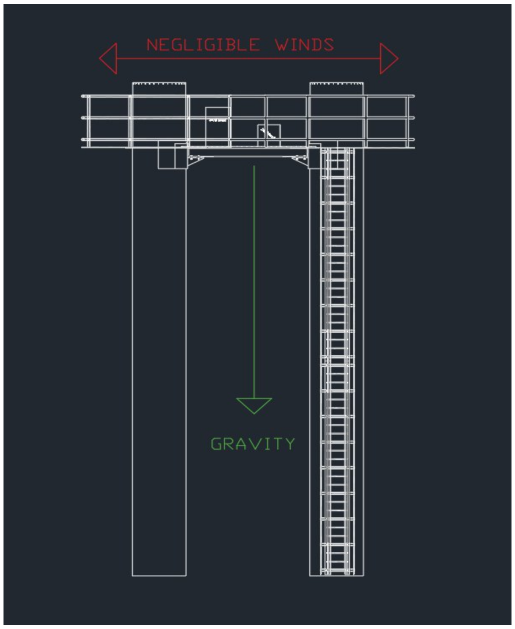

Figure 2: Case Study 2 Side View

Case 2: Worst Conditions

Background: Flare stacks and surrounding structures have many connections to be considered. Especially considering the necessity of reliable support of flaring systems.

Scenario: The beam is being analyzed on a hot, windy day in Tulsa Oklahoma. There is up to 2.625 inches of movement in the flare stacks. The ambient temperature is above 100°F. Heavy flaring occurs so the beams and surrounding structures do not have ample time to cool. The live load is 75psf, including a 357lb load roughly 4ft from the center of the left flare center, and a 234lb load roughly 4.5ft from the right flare center. The flare stack shell thickness is 5/16 inches. There are imposed wind forces of 1615lbf perpendicular to the long side of the beams. The structure also experiences oscillations once every 13 minutes.

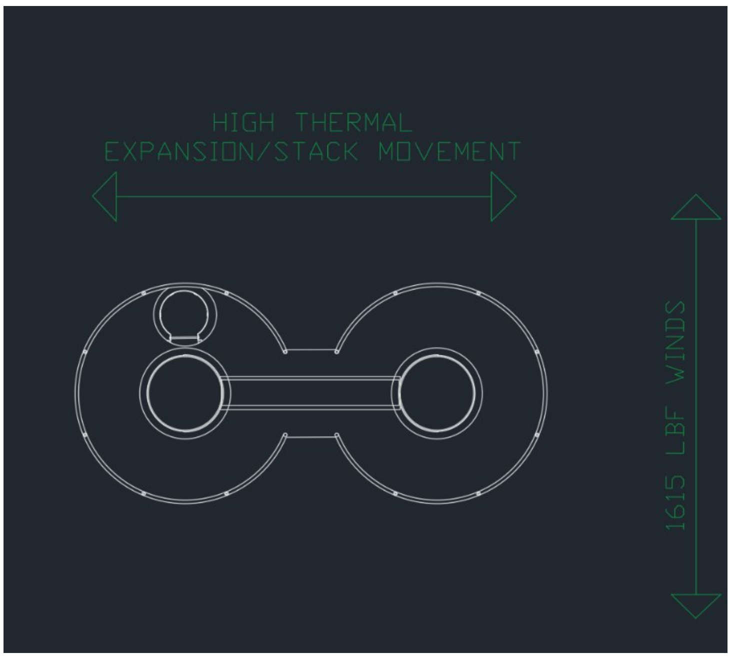

Figure 3: Case Study 2 Top View

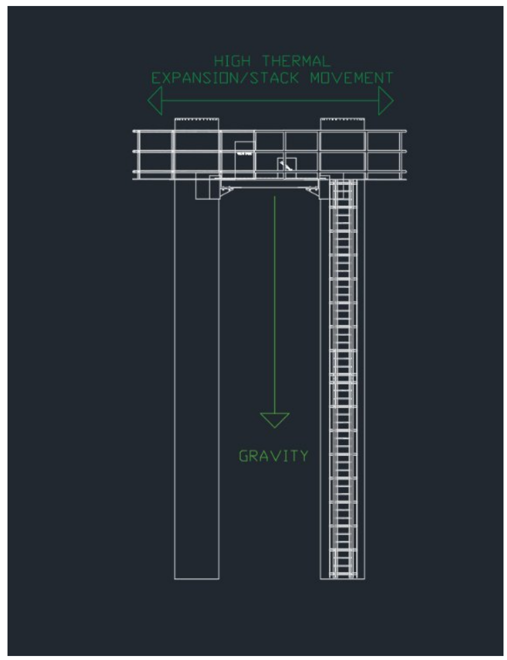

Figure 4: Case Study 2 Side View

Findings: The beam is sufficiently sized to support the live load and added forces. Slotted holes in the beams will be necessary to accommodate thermal expansion and flare stack movement.

Design Calculations

Load Analysis

Case 1: Ideal Conditions, Beam-1 Analysis

Clearcalcs.com (ii) provides a useful beam calculation tool with illustrations of the load, shear, and moment and deflection diagrams tailored to specified loads and end conditions. The results provided by this calculator will be compared to the calculations completed by hand.

Online Calculator Results

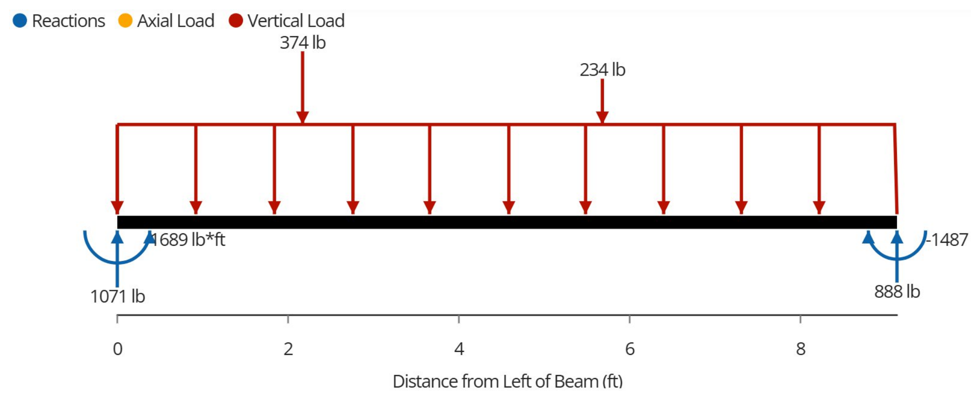

Figure 5: Loading Diagram

Figure 5: Loading Diagram illustrates the load conditions on Beam-1: 2 point loads and a uniform distributed load. The reactions forces and moments are also displayed.

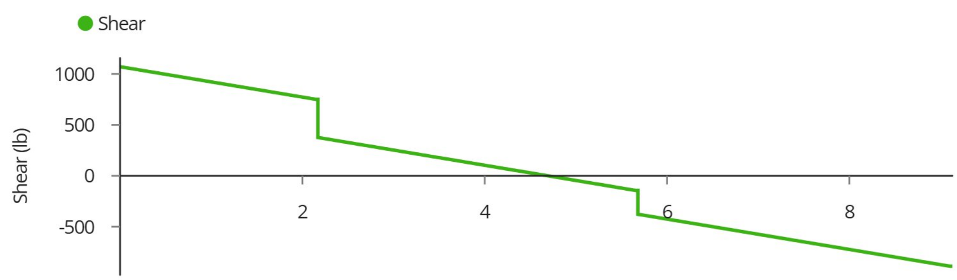

Figure 6: Shear Diagram

Figure 6: Shear Diagram illustrates the shear conditions created at each end. Greater than 1000 lbs of shear force at the left end and at the other end greater than 500 lbs of shear force. The shear is in the same direction relative to the Y axis, but is plotted relative to the normal direction at the end of the beam. This results in the left side as positive values and the right side as negative values.

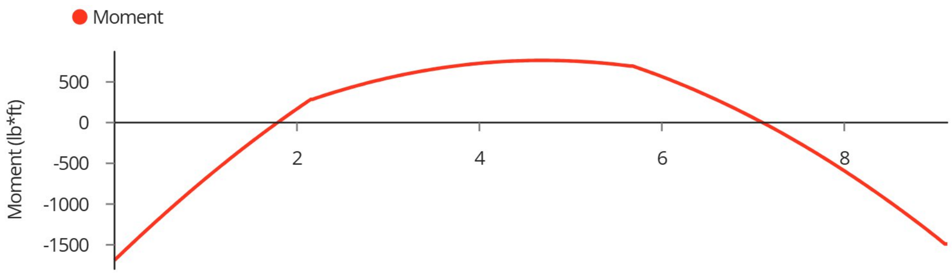

Figure 7: Moment Diagram

Figure 7: Moment Diagram illustrates the moments created at each end. The moments at each end are opposite to one another in direction, but are plotted relative to the side of the beam they are on. The left generates greater than 1500 ft-lbs while the right generates about 1500 ft-lbs.

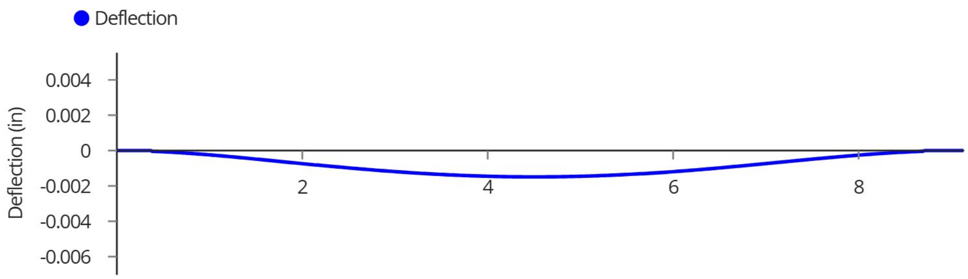

Figure 8: Deflection Diagram

Figure 8: Deflection Diagram illustrates the resulting deflection given the initial load conditions. The deflection is measured in inches and has a maximum of slightly less than 0.002 and is downward.

The results are tabulated below:

Table 3: Resulting Load Conditions on Beam-1

Reaction R_1 (lb)	Reaction R_2 (lb)	Shear V_1 (lb)	Shear V_2 (lb)	Moment M_1 (ft-lb)	Moment M_2 (ft-lb)	Deflection δ (in)
1071	888	1071	-888	-1689	1487	-0.00149

Beam-1 experiences reaction forces of 1071 lb at support A and 888 lb at support B. Shear forces are 1071 lb at the left end and -888 lb at the right end, the sign change is the result of the change in normal direction from one end to the other. The bending moments are -1689 ft-lb at the left end and 1487 ft-lb at the right end, showing resistance to applied loads. The beam's maximum deflection is -0.00149 in, indicating minimal downward displacement.

Hand Calculations

The hand calculations were performed using the superposition principle, which allows each load to be analyzed independently before combining their effects to determine the total load condition. In Case 1, the system is assumed to be in static equilibrium, and the reaction forces and moments were derived accordingly using superposition. The formulas used were sourced from *Shigley's Mechanical Engineering Design* textbook.

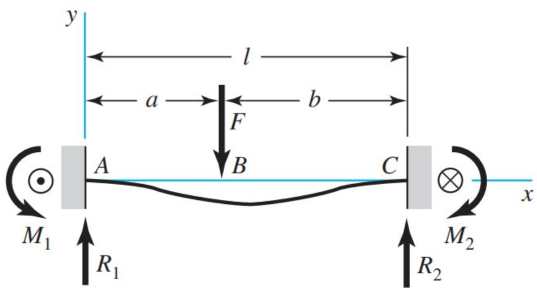

Figure 9: Appendix A-9, Fixed Supports intermediate load

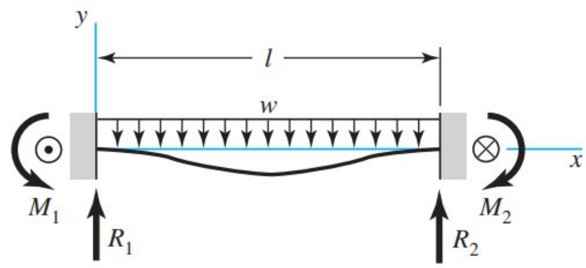

Figure 10: Appendix A-9, Fixed Supports uniform load

- Formulas used to calculate the reaction forces:

Fixed Supports – Intermediate Load (*Figure 9*)

Equation 1: Reaction 1

$$R_1 = \frac{Fb^2}{l^3}(3a + b)$$

Equation 2: Reaction 2

$$R_2 = \frac{Fa^2}{l^3}(3b + a)$$

Fixed Supports – Uniform Load (*Figure 10*)

Equation 3: Reactions

$$R_1 = R_2 = \frac{wl}{2}$$

Table 4: Beam-1 Reaction Forces

Reaction Forces	Superposition					
Due to:	P_1 (lbf)	+	P_2 (lbf)	+	w (lbf)	= Reaction (lbf)
Using Moment at pt. 1: At R_1	320.52		74.79		675	1070.32
At R_2	53.48		159.21		675	887.68
sum	374.00		234.00		1350	1958.00

Table 2 shows the beam at the left fixed point experiences a reaction force of 1070.32 lbf, comprised of 320.52 lbf from P_1, 74.79 lbf from P_2, and 675 lbf from the distributed load. At the right fixed point, the reaction force is 887.68 lbf, comprised of 53.48 lbf from P_1, 159.21 lbf from P_2, and 675 lbf from the distributed load. The total vertical load on the beam is 1958 lbf, confirming equilibrium.

- Formulas used to calculate the shear forces:

Fixed Supports – Intermediate Load
(*Figure 9*)

Equation 4: Shear Force AB

$$V_{AB} = R_1$$

Equation 5: Shear Force BC

$$V_{BC} = -R_2$$

Fixed Supports – Uniform Load
(*Figure 10*)

Equation 6: Shear Force

$$V = \frac{w}{12}\left(6lx - 6x^2 - l^2\right)$$

Table 5: Beam-1 Shear Forces

Beam-1	Superposition					
Shear Forces	P_1 (lbf)	+	P_2 (lbf)	+	w (lbf)	= Reaction (lbf)
V_1	320.52		74.79		675	1070.32
V_2	-53.48		-159.21		-675	-887.68

Table 3: Beam-1 Shear Forces, the shear force vector is pointing opposite for each end of the beam. The shear force at the left end of the beam is 1070.32 lbs (upward) and at the right end is 887.68 lbs (downward).

- Formulas used to calculate the moment:

Fixed Supports – Intermediate Load
(*Figure 9*)

Equation 7: Moment 1

$$M_1 = \frac{Fab^2}{l^2}$$

Equation 8: Moment 2

$$M_2 = \frac{Fa^2b}{l^2}$$

Fixed Supports – Uniform Load
(*Figure 10*)

Equation 9: Moments

$$M_1 = M_2 = \frac{wl^2}{12}$$

Table 6: Beam-1 Moments

Beam-1	Superposition					
Moments	P_1 (ft-lbf)	+	P_2 (ft-lbf)	+	w (ft-lbf)	= Reaction (ft-lb)
M_1	-471.63		-189.27		-1026.56	-1687.46
M_2	147.32		312.39		1026.56	1486.27

Table 4: Beam-1 Moments shows the moment effect of the applied loads. The moment at the left end of the beam, M_1, is counterclockwise and 1687.46 ft-lb, and at the right end, M_2, clockwise and 1486.27 ft-lb.

- Formulas used to calculate the deflection:

Fixed Supports – Intermediate Load
(*Figure 9*)

Equation 10: Deflection 1

$$P_1 = \delta_{BC} = \frac{Fa^2 (l-x)^2}{6EIl^3} [(l-x)(3b+a) - 3bl]$$

Equation 11: Deflection 2

$$P_2 = \delta_{AB} = \frac{Fb^2 x^2}{6EIl^3} [x(3a+b) - 3al]$$

Fixed Supports – Uniform Load
(*Figure 10*)

Equation 12: Maximum Deflection

$$\delta_{max} = -\frac{wl^4}{384EI}$$

Table 7: Beam-1 Deflection

Beam-1	Superposition						
Deflection	P_1 (ft)	+	P_2 (ft)	+	w (ft)	=	δ (in)
δ	-2.05E-05		-2.35E-05		-7.99E-05		-1.49E-03

Table 5 shows P_1 produces a maximum deflection to the right of the point load, thus δ_{BC} formula was used~~ to determine~~~~Maximum.~~ P_2 is positioned right of center, thus the maximum deflection occurs to the left of the point load near the center. δ_{AB} formula was used. The maximum deflection of Beam-1 is ~~calculated as~~ 0.00149 inches downward. The magnitude is very small and would likely be considered insignificant.

Direct comparison between results:

Table 8: Beam-1 Online Beam Calculator vs Hand Calculations

Beam-1	Online Calculator	Hand Calculations	Units	Difference
Reaction force R_1	1071	1070.32	lb	0.68
Reaction force R_2	888	887.68	lb	0.32
Shear force V_1	1071	1070.32	lb	0.68
Shear force V_2	-888	-887.68	lb	0.32
Moment M_1	1689	1687.46	ft-lb	1.54
Moment M_2	1487	1486.27	ft-lb	0.73
Deflection δ	-0.00149	-0.00149	in	0

The differences shown in Table 6 can be attributed to the online calculator appearing to round off numbers. However, where the deviation occurs, the hand calculations fall within an acceptable margin of error.

Case 1: Ideal Conditions, Beam-2 Analysis

Similar procedure was conducted on the second beam. The live load is assumed to be the only force acting directly on the beam resulting in one uniform distributed load across the beam.

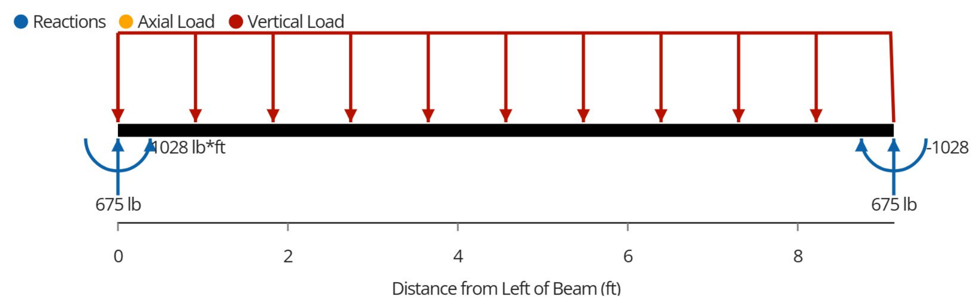

Figure 11: Loading Diagram

Figure 11: Loading Diagram illustrates the load conditions on Beam-2: a uniform distributed load. The reactions forces and moments are also displayed.

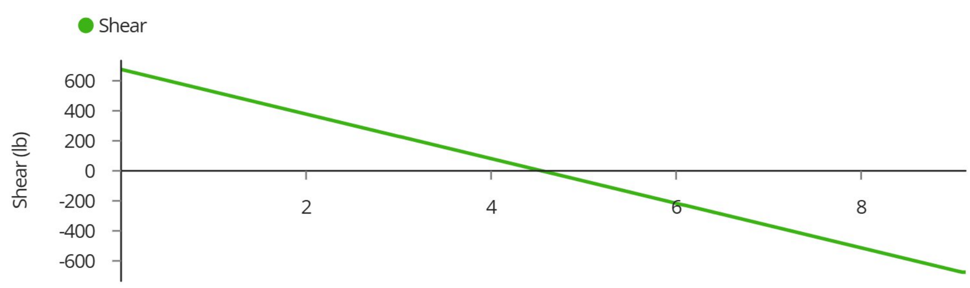

Figure 12: Shear Diagram

Figure 12: Shear Diagram illustrates the shear conditions created at each end. The uniform distributed load generates a shear reaction greater than 600 lb force at each end.

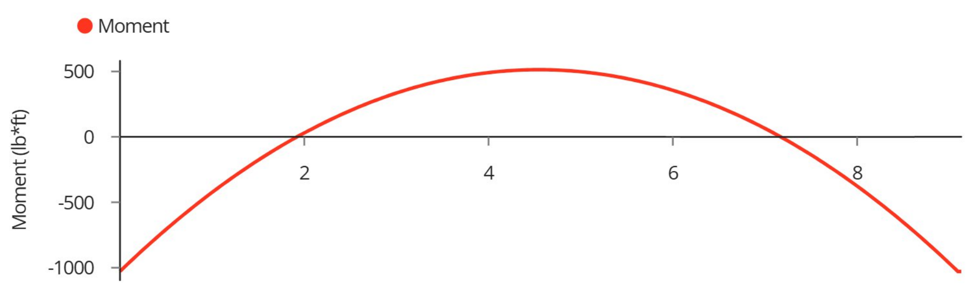

Figure 13: Moment Diagram

Figure 13: Moment Diagram illustrates the moments created at each end. The distributed load generates a symmetrical moment at each end of the beam. The magnitude of the moments are slightly greater than 1000 ft-lbs.

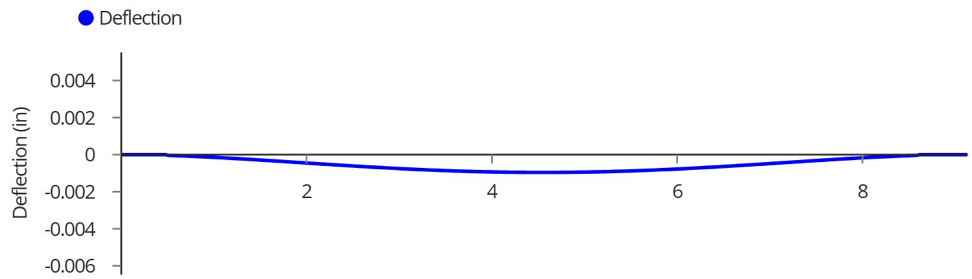

Figure 14: Deflection Diagram

Figure 14: Deflection Diagram illustrates the resulting deflection generated by the distributed load. The deflection is less than 0.001 inches downward.

The results have been tabulated below:

Table 9: Resulting Load Conditions on Beam-2

Reaction R_1 (lb)	Reaction R_2 (lb)	Shear V_1 (lb)	Shear V_2 (lb)	Moment M_1 (ft-lb)	Moment M_2 (ft-lb)	Deflection δ (in)
675	675	675	-675	1028	-1028	-0.000961

Table 7 presents the resulting load conditions on Beam-2, including reaction forces, shear forces, moments, and deflection. The reactions at both supports (R_1 and R_2) are 675 lb each. The shear forces (V_1 and V_2) are 675 lb and -675 lb, respectively. The moments at two locations (M_1 and M_2) are 1028 ft-lb and -1028 ft-lb. The beam experiences a small deflection of -0.000961 in, indicating minimal deformation under the applied loads.

Hand Calculations

The values below were calculated using formulas from Shigley's Mechanical Engineering Design textbook Appendix A-9 Fixed Supports – Uniform Load.

Table 10: Beam-2 Tabulated Hand Calculation Results

Reaction R_1 (lb)	Reaction R_2 (lb)	Shear V_1 (lb)	Shear V_2 (lb)	Moment M_1 (ft-lb)	Moment M_2 (ft-lb)	Deflection δ (in)
675	675	675	-675	1026.56	-1026.56	-0.000958

Direct comparison between results:

Table 11: Beam-2 Online Beam Calculator vs Hand Calculations

Beam-1	Online Calculator	Hand Calculations	Units	Difference
Reaction force R_1	675	675	lb	0
Reaction force R_2	675	675	lb	0
Shear force V_1	675	675	lb	0
Shear force V_2	-675	-675	lb	0
Moment M_1	1028	1026.56	ft-lb	1.44
Moment M_2	-1028	-1026.56	ft-lb	1.44
Deflection δ	-0.000960	-0.000958	in	~0

Table 9 shows a comparison between the online beam calculator and hand calculations for Beam-2. The results are identical values for reaction forces, shear forces, and deflection, with only a minor difference (1.44 ft-lb) in bending moments. This small discrepancy is likely due to rounding by the online calculator.

Case 2: Worst-Case Scenario

All loads from Case 1 are still present, with an additional 1,615 lbf traverse wind load applied to the system. The worst-case scenario assumes this load is applied perpendicular to the beam's length, maximizing surface area exposure and generating drag on the stack. The force is considered uniformly distributed on the windward side. As in Case 1, the results from the online beam calculator will be compared to hand calculations.

The results of the online calculator:

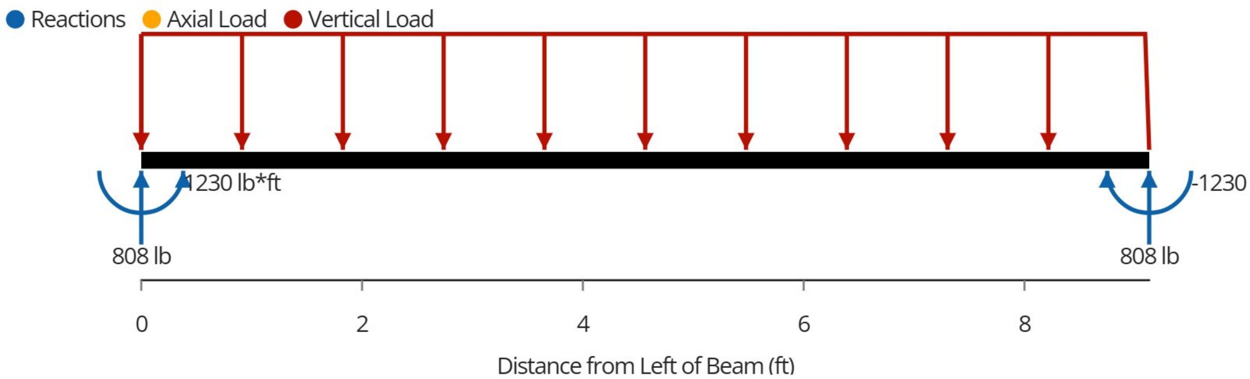

Figure 15: Loading Diagram

Figure 15: Loading Diagram illustrates the load conditions: a uniform distributed load. The reactions forces and moments are also displayed.

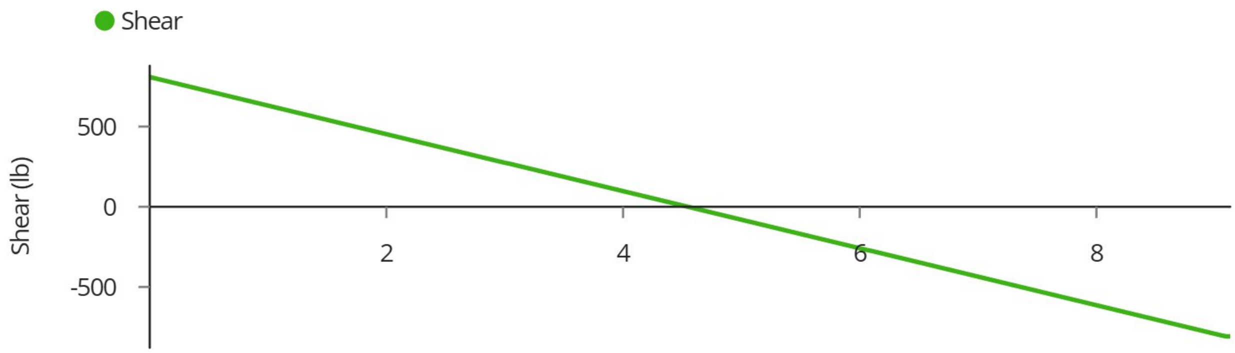

Figure 16: Shear Diagram

Figure 16: Shear Diagram illustrates the shear conditions created at each end. The uniform distributed load generates a shear reaction greater than 500 lb force at each end.

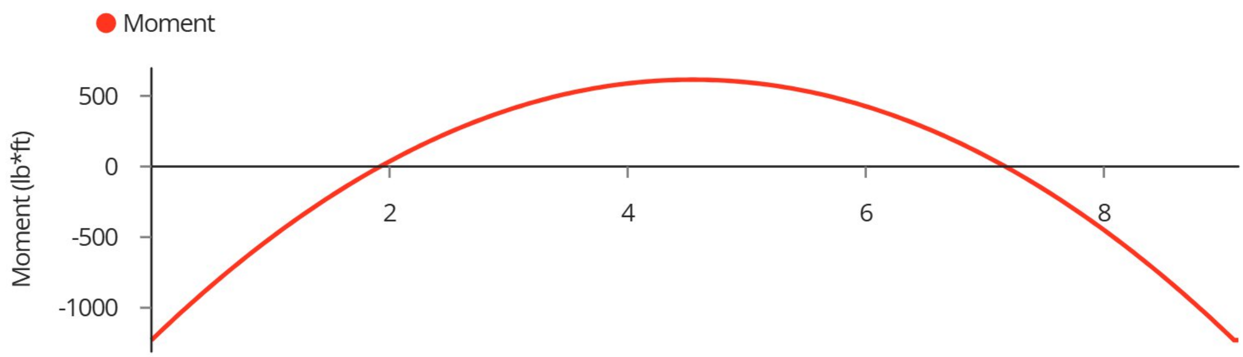

Figure 17: Moment Diagram

Figure 17: Moment Diagram illustrates the moments created at each end. The distributed load generates a symmetrical moment at each end of the beam. The magnitude of the moments are greater than 1000 ft-lbs.

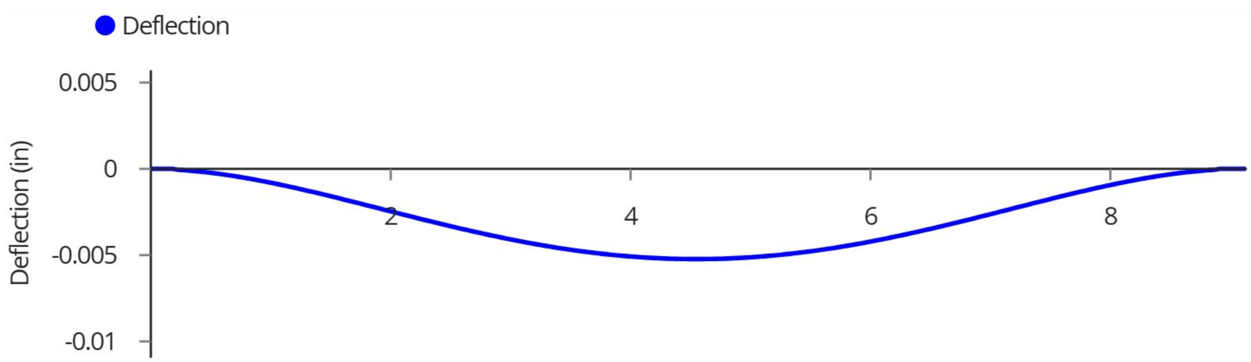

Figure 18: Deflection Diagram

Figure 18: Deflection Diagram illustrates the resulting deflection generated by the distributed load. The deflection is about 0.005 inches downward.

The results have been tabulated below:

Table 12: Online Calculator Results

Reaction R_1 (lb)	Reaction R_2 (lb)	Shear V_1 (lb)	Shear V_2 (lb)	Moment M_1 (ft-lb)	Moment M_2 (ft-lb)	Deflection δ (in)
808	808	808	-808	1230	-1230	-0.00523

Table 10 presents the resulting load conditions, including reaction forces, shear forces, moments, and deflection. The reactions at both supports (R_1 and R_2) are 808 lb each. The shear forces (V_1 and V_2) are 808 lb and -808 lb, respectively. The moments at two locations (M_1 and M_2) are 1230 ft-lb and -1230 ft-lb. The beam experiences a small deflection of -0.00523 in, indicating minimal deformation under the applied loads.

Hand Calculations

The values below were calculated using formulas from Shigley's Mechanical Engineering Design textbook Appendix A-9 Fixed Supports – Uniform Load.

Table 13: Tabulated Hand Calculation Results

Reaction R_1 (lb)	Reaction R_2 (lb)	Shear V_1 (lb)	Shear V_2 (lb)	Moment M_1 (ft-lb)	Moment M_2 (ft-lb)	Deflection δ (in)
807.5	807.5	807.5	-807.5	1228.07	-1228.07	-0.005217

Direct comparison between results:

Table 14: Beam-2 Online Beam Calculator vs Hand Calculations

Beam-1	Online Calculator	Hand Calculations	Units	Difference
Reaction force R_1	808	807.5	lb	0.5
Reaction force R_2	808	807.5	lb	0.5
Shear force V_1	808	807.5	lb	0.5
Shear force V_2	-808	-807.5	lb	0.5
Moment M_1	1230	1228.07	ft-lb	1.93
Moment M_2	-1230	-1228.07	ft-lb	1.93
Deflection δ	-0.00523	-0.00521	in	~0

Table 12 shows a comparison between the online beam calculator and hand calculations for Beam-2. The results are similar values for reaction forces and shear forces, with a difference of 0.5 lb. The deflection is basically the same, and the bending moments have a minor difference of 1.93 ft-lb. This small discrepancy is likely due to rounding by the online calculator.

Bolt Calculations

The bolts must withstand the worst-case scenario conditions (Case 2). As outlined in the ***Case Studies*** section, Case 2 assumes a traverse wind load on the system, generating shear stress on the fasteners and causing stack oscillation.

The images below illustrate the fastener assemblies:

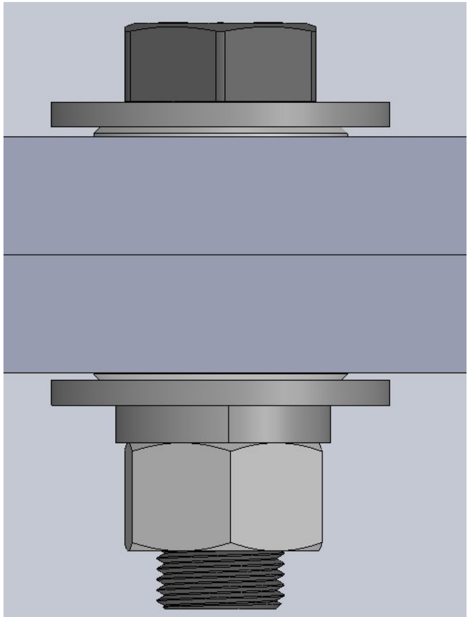

Figure 19: Side View Bolt Assembly

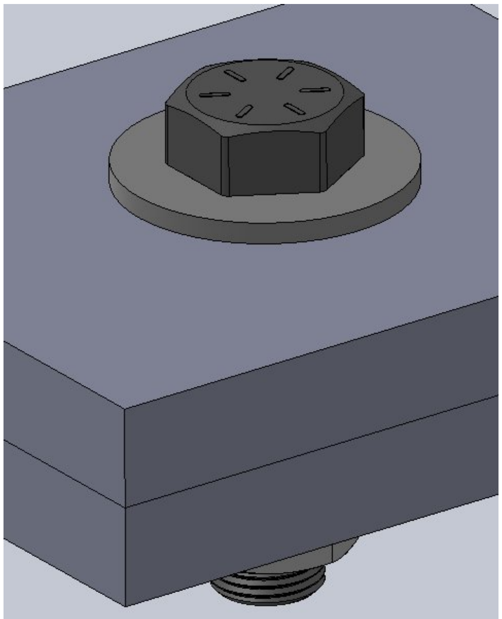

Figure 20: Isometric View of Bolt Assembly

Assembly Items

- Bolt
- Washer
- Spacer
- Washer
- Lock washer
- Nut

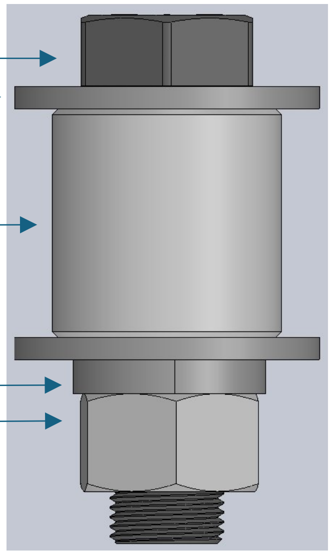

Figure 21: Hardware Design

Design Considerations

The fastener assembly design accounts for factors such as thermal expansion and stack oscillation. The top plate represents the beam spanning between the two stacks, while the bottom plate represents the stack collar component. The bolt and nut clamp onto the spacer between the washers. A deliberate gap, created by the spacer, prevents the fastener assembly from clamping the plates together. This gap allows the beam to move in response to environmental changes throughout the year. Additionally, the spacer increases the fastener's shear strength by enhancing the cross-sectional area.

Requirements for the Bolt Assembly

1. Bolt tension must be sufficient to prevent the fasteners from loosening due to vibration or movement.
2. Shear strength of the fastener assembly must be adequate to withstand the maximum stress conditions defined in *Case 2: Worst Conditions*.

Determining Preload Required to Prevent Back Off

The torque required to prevent the nut from backing off and loosening due to vibration is a function of the torque coefficient (K) to account for friction in the threads, the required preload (F_i), and the bolt diameter (d):

Equation 13: Torque

$$T = K F_i d$$

The required preload is a function of the proof strength (S_p) and the tensile stress area (A_t). Both values can be attained from tables provided in Shigley's Mechanical Engineering Design textbook (i).

Equation 14: Pre-loading Force

$$F_i = A_t S_p$$

The results are tabulated below:

Table 15: Requirements to Secure Bolt

Torque Coefficient	Preload (lb)	Bolt Diameter (ft)	Proof Strength (psi)	Tensile Stress Area (in^2)	Torque Required ft-lb
0.2	2853.5	0.06	85000	0.373	356.68

The total torque required to meet the preload requirements is 357 ft-lb. Although using a torque wrench is not the most reliable method to preload a bolt, it is a more practical method in many situations. The more reliable method is to measure the bolts elongation with a micrometer. If there were only a single bolt fastening the beam to the stack collar, then it may require a more rigorous measurement of the preload.

Effects of Traverse load on Bolts

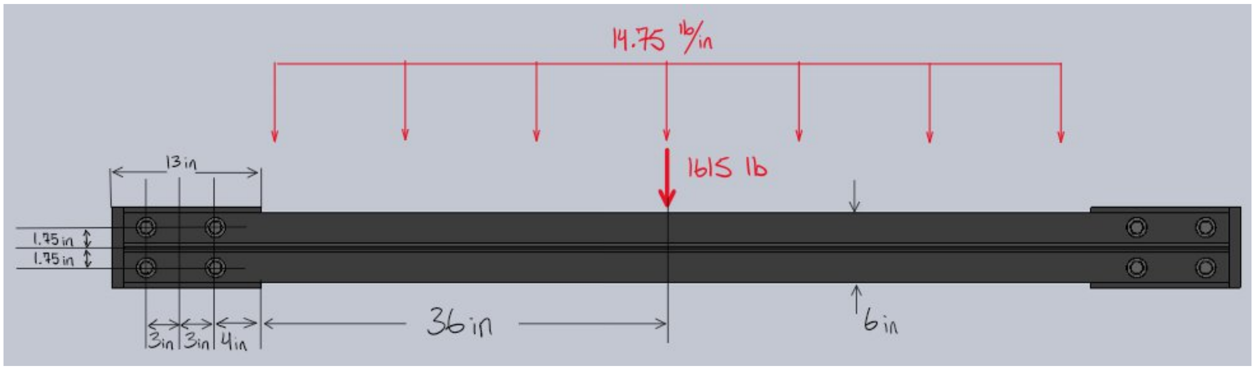

Figure 22: Free Body Diagram of Beam

Figure 22 illustrates the 1615 lb wind load acting on the beam. It is assumed that this beam absorbs the entire wind load, serving as a windbreaker for the second beam, effectively minimizing its effects on the second beam. The load is uniformly distributed along the surface of the beam where contact occurs.

Table 11 presents the shear and moment forces at each end of the beam:

- Shear force: V = 807.5 lb
- Moment: M = 1228.07 ft-lb

The focus is on identifying which bolts experience the highest shear stress.

The primary shear load per bolt (F′) is determined by dividing the total shear force (V) by the number of bolts (n):

Equation 15: Shearing Load per Bolt

$$F' = \frac{V}{n}$$

The secondary shear load per bolt (F'')(F″) is ~~written as a function of~~calculated based on the moment (M) and the radial distance (r) from the centroid to the bolt center~~ of the bolt (r), which is the same for each bolt:¶~~
. Since the bolts are symmetrically positioned, this is expressed as:

Equation 16: Secondary Shearing Load per Bolt

$$F'' = \frac{M}{4r}$$

SOLIDWORKS was used to determine the shear resultant load on each bolt. Below is a diagram illustrating these forces:

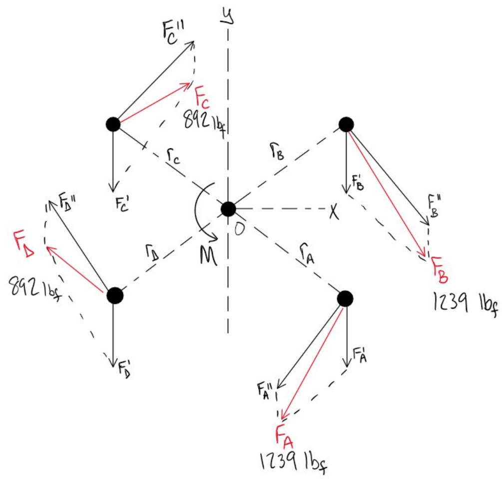

Figure 23: Shear Load Resultant Diagram

The shear load results are tabulated below:

Table 16: Shear Load Analysis

Shear Load about point *o* (lb)	Moments about *o* (ft-lb)	Primary (F') (lb)	Secondary (F'') (lb)	Distance (r) (in)	Resultant (lb)
807.5	1228.07	201.9	1060.8	3.47	$F_A = F_B = 1239$ $F_C = F_D = 892$

Based on the results presented in Table 14, the highest resultant shear loads occur at bolts A and B, each experiencing a force of 1,239 lb. This is significantly higher than the shear loads at Bolts C and D, which are 892 lb each. The primary shear load per bolt (F′) is 201.9 lb, derived from the total shear force (807.5 lb) divided among the bolts. The secondary shear load per bolt (F′′) is 1060.8 lb, which is influenced by the moment (1228.07 ft-lb) and the radial distance (3.47 in). These values are combined using the parallelogram rule to determine the resultant forces acting on each bolt. From these calculations, it is evident that bolts A and B endure the highest shear stress, making them the critical points in the system that may require additional reinforcement or consideration in the design.

The bolt and spacer are simplified and considered a solid shaft 1.5 inches in diameter. The body area of each fastener is:

Equation 17: Area of Circle

$$A = \frac{\pi(d^2)}{4}$$

We want to analyze the places that are most likely to fail. Thus, the critical shear load (shown in Table 14) will be used to calculate the shear stress (τ) on bolts A and B.

Equation 18: Shear Stress

$$\tau = \frac{F}{A} = \frac{1239}{1.767} = 701.19\ psi$$

The factor of safety can be calculated as a function of the von Mises shear stress per applied shear stress:

Equation 19: Factor of Safety

$$n_d = \frac{0.577 S_y}{\tau} = \frac{0.577(92000)}{701.19} = 75$$

The bearing stress occurs where the bolt is pressing against the hole walls. Since each member is the same thickness, the bearing area (A_b) will be a function of both member thicknesses (t) and the diameter (d) of the hole:

Equation 20: Bearing Area

$$A_b = td$$

The bearing stress as a function of the force and bearing area:

Equation 21: Bearing Stress

$$\sigma = -\frac{F}{A_b}$$

Below are the tabulated results calculating the bearing stress:

Table 17: Bearing Stress

Thickness (in)	Diameter (in)	Bearing Area (in^2)	Force (lb)	Bearing Stress (psi)
2	1.5	3	1239	413

Table 15 presents the calculated bearing stress based on a material thickness of 2 inches and a hole diameter of 1.5 inches, resulting in a bearing area of 3 square inches. With an applied force of 1,239 pounds, the corresponding bearing stress is determined to be 413 psi.

The critical bending stress in the bar can be assumed to occur at bolts A and B. The formula for the critical bending stress is a function of the moment (M) at bolts A and B, the second moment of inertia (I), and the distance (c) from the center to the outer most edge of the beam.

Equation 22: Bending Stress

$$\sigma = \frac{Mc}{I}$$

Where the Moment at bolts A and B and the second moment of inertia in traverse direction are:

Equation 23: Moment

$$M = Force\ (F) \times Distance\ (D),$$

Equation 24: Inertia

$$I = \left\{2\left(\frac{tw^3}{12}\right) + \left[\frac{(h-2t)\,(t^3)}{12}\right]\right\} - 2\left[\frac{td^3}{12} + \bar{d}^2 A\right]$$

Table 18: Critical Bending Stress Results

Thickness (t) (in)	Width (w) (in)	Height (h) (in)	Diameter (d) (in)	Area (in^2)	Distance (c) (in)	Distance ($\bar{d}$) (in)	Moment (in-lb)	Inertia (I) (in^4)	Bending Stress (σ) psi
1	6	8	1.5	3	3	1.75	32,300	26.75	3,588.8

Welding Calculations

To ensure the structural integrity of the connection between the beam section and the stack, welding calculations were performed based on a fillet weld configuration using carbon steel. The primary goal of these calculations is to verify that the weld is capable of supporting the applied load with an appropriate safety margin. Weld callouts will be upsized to the next standard size for the sake of easy manufacturing, standardizations, and an improved safety factor considering the human element of welded components.

Known Parameters

The known design parameters are as follows:

- Weld type: Fillet weld
- Total downward force (F): 1958 lbf
- Radius of collar (r): 22 inches
- Weld length (L): 138.23 inches
- Material: Carbon Steel
  - Yield strength (S_y) = 36,000 psi
- Design safety factor (n): 3

Weld Size

To determine the weld size (W), we use the following formula for fillet welds:

Equation 24: Weld Size

$$W = \sqrt{\frac{F}{0.707 * S_y * L}}$$

Stress in the Weld

After finding the weld size, we evaluate the stress developed in the weld under the applied load. The stress is calculated using the following basic equation:

Equation 25: Stress

$$Stress = \frac{F}{A}$$

Equation 26: Throat Area

$$A = W * L$$

Parameter	Calc	Result	Units
Bracket	1958 / 2	979	lbf
Allowable Shear Stress	36000 / (√2 × 3)	~12000	psi
Weld Length (Bracket to Collar)	8 in × 2 = 16 in	16	in
Required Throat Area (Bracket)	979 / 12000	0.0816	in^2
Effective Throat	0.0816 / 16	0.0051	in
Minimum Weld Size	0.0051 / 0.707	0.0072	in
Specified Weld Size	**1/8**	0.125	in

Table 17: Bracket Weld Data

Parameter	Calc	Result	Units
Collar	1958	1958	lbf
Weld Length	2π × 22 ≈ 138.23	138.23	in
Required Throat Area	1958 / 12000	0.1632	in^2
Effective Throat	0.1632 / 138.23	0.00118	in
Minimum Weld Size	0.00118 / 0.707	0.00167	in
Specified Weld Size	**1/32**	0.03125	in

Table 18: Collar Weld Data

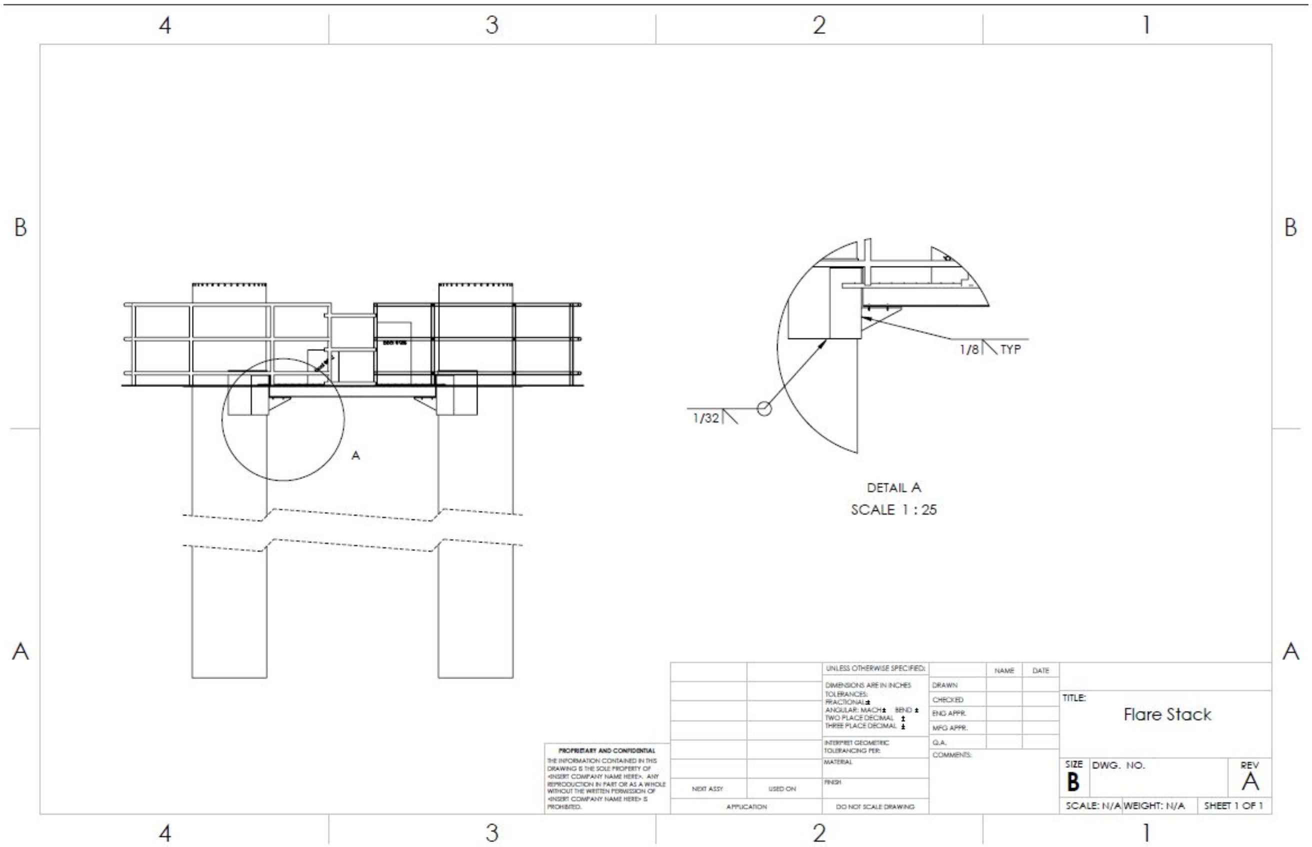

Figure 24: Weld Callouts

Oscillation Analysis

Considering the wind loading, oscillating conditions and time interval to complete one revolution; this creates a marginal system for analysis and how the conditions affect the reinforcement system and the evaluation of the entire system. Under these conditions, the assessment to see if the final design has the ability to endure external factors. Below are assumptions that will simplify the model and the series of calculations below.

Assumptions:

- The refinery stacks will move in unison for simplicity.
- The wind direction will remain constant.
- The wind load is horizontal making the lift coefficient negligible.
- The wind load is only applicable at the platform, the height of the refinery stacks will not be accounted for.
- The wind velocity will remain constant
- The refinery stack will be treated as a spring-damper system.
- The system will be harmonic.

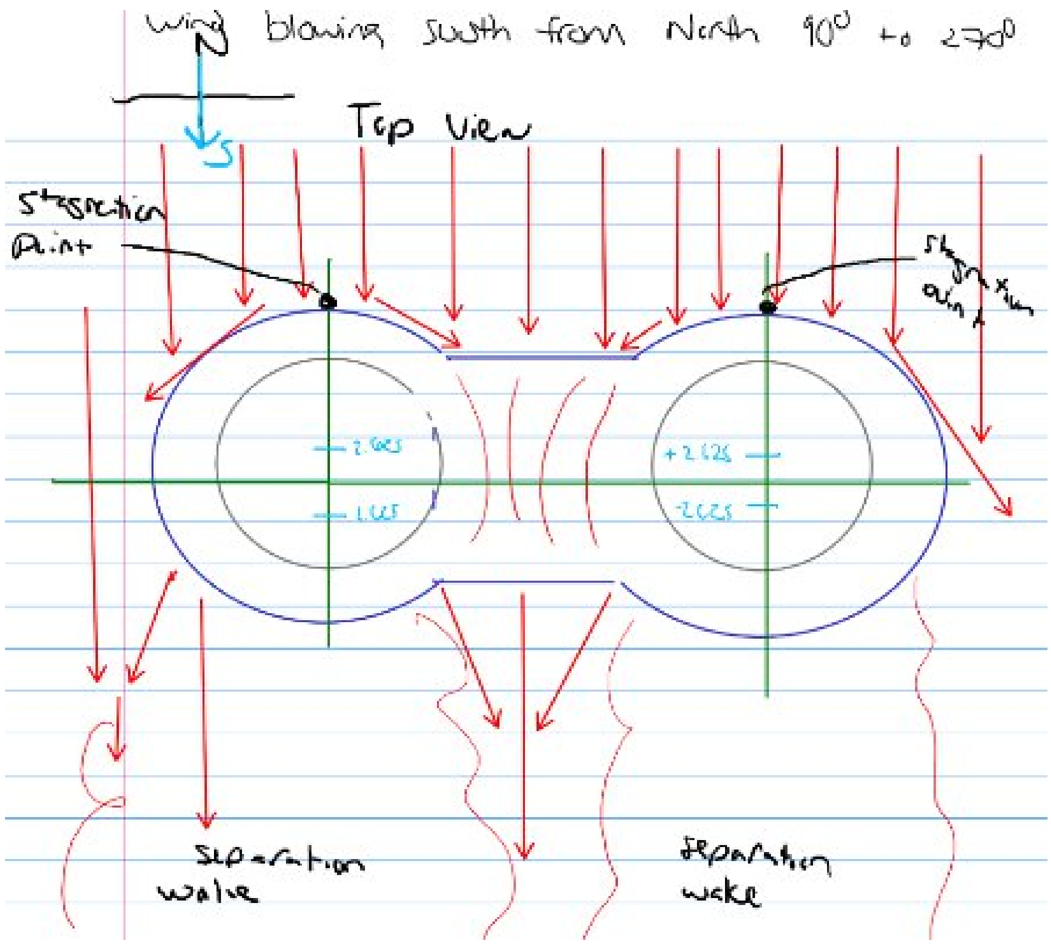

Figure 24: Wind Velocity streamlines from North to South

In figure 24, illustrate the top view planar face of where the wind blowing from North to South. The red lines are velocity vector field, and it shows the transition from laminar flow to turbulent flow. The swivelly red line represents the separation and wake created from the structure. The flow is initially assumed to be inviscid flow, and once it becomes turbulent it becomes viscous flow. There will be a lot of circulation and vorticity within in between the stacks. The figure also, shows the oscillation range at the origin of each refinery stack. The table below displays the initial conditions and will be implemented into the overall calculations.

Table 19: Initial Conditions

Initial Conditions		
Wind Load	Force(wind)	1615 lbf
Time	t	780 s(13 min)
Amplitude	A	2.625 in

Equations:

Equation 27: Newton's Second Law

$$\sum F = ma$$

Equation 28: Moment

$$\sum M = F \cdot d$$

Equation 29: Drag Force

$$F_d = \frac{1}{2} \cdot C_d \cdot A_t \cdot \rho_{air} \cdot V_{wind}^2$$

Equation 30: Amplitude

$$A = \frac{F_w}{m \cdot \sqrt{\left(\left(1 - \left(\frac{\omega_0}{\omega}\right)^2\right)^2 - \left(2\zeta \frac{\omega_0}{\omega}\right)^2\right)}}$$

Equation 31: Natural Frequency

$$\omega_o = \frac{1}{2\pi} \sqrt{\frac{k}{m}}$$

Equation 32: Damped Natural Frequency

$$\omega_d = \omega_{n\sqrt{1-\zeta^2}}$$

Equation 33: Damping Ratio

$$\zeta = \frac{c}{2\sqrt{mk}}$$

Equation 34: Differential Equation of Motion

$$m\frac{d^2x}{dt^2} + c\frac{dx}{dt} + kx = F(t)$$

Equation 35: Harmonic Equation for Displacement

$$x(t) = A\cos(\omega_d \cdot t + \phi)$$

Equation 36: Reynold's Number

$$Re = \frac{\rho V_\infty x}{\mu}$$

Equation 37: Drag Coefficient

$$c_d = \frac{D'}{q_\infty c}$$

Equation 38: Dynamic Pressure

$$q_\infty = \frac{1}{2} \cdot \rho \cdot V^2$$

Equation 39: Stiffness

$$k = \frac{48EI}{L^3}$$

Table 18 below provides applicable constant values needed to complete the calculations.

Table 20: Constants

Constants		
Density	Rho(air)	0.002377 slug/ft^3
Mass	m	33852.36 lbm
Gravitational Acceleration	g	32.2 ft/s^2
Dynamic Viscosity	Mu(air)	0.3766(10^-6) (lbf*s)/ft^2
A36 Modulus of Elasticity	E(A36)	4.18(10^9) psf

Table 21: Material Properties and Dimensions

Material Properties & Refinery Stack & Support System Dimensions		
I-Beam Width	B	0.5 ft
I-Beam Height	H	0.67 ft
I-Beam Length	L	9.13 ft
I-Beam Fillet Radius	r	0.04 ft
I-Beam Web Thickness	a	0.08 ft
I-Beam Flange Thickness	e	0.08 ft
Refinery Stack Thickness	T(shell)	0.026 ft
Refinery Stack Outer Diameter	D(out)	3.5 ft
Platform Outer Diamter	X(out)	10 ft
Platform Inner Diameter	X(in)	4 ft
Platform Rectangular Width	W(rect)	2 ft
Platform Thickness	t(platform)	0.04ft (assumed)

Table 19 provides applicable dimension of the I-beams, platform, refinery stack, and all other components were taken into account for simplicity.

Table 22: Structural Area and Volume Calculations

Area and Volume Calculations		
I-Beam Area XZ plane	A(I-beam),(xz)	0.13 ft^2
I-Beam Area YZ plane	A(I-Beam),(yz)	4.99 ft^2
I-Beam Area XY plane	A(I-Beam),(xy)	4.01 ft^2
I-Beam Volume	V(I-Beam)	1.154 ft^3
Collar Area	A(collar)	8.66 ft^2
Collar Volume	V(collar)	0.1996 ft^3
Stack Area XY Plane	A(stack),(xy)	0.46 ft^2
Stack Area XZ plane	A(stack),(xz)	7.743 ft^2
Stack Volume	V(stack)	15.487 ft^3
Platform Area XY plane	A(platform),(xy)	116.55 ft^2
Platform Area XZ plane	A(platform),(xz)	2.16 ft^2
Platform Volume	V(platform)	4.662 ft^3

In table 20, the tabulations of planar area for certain components and the volume. All other components were assumed to be negligible for simplicity. Some of the values were provided from the SolidWorks Model.

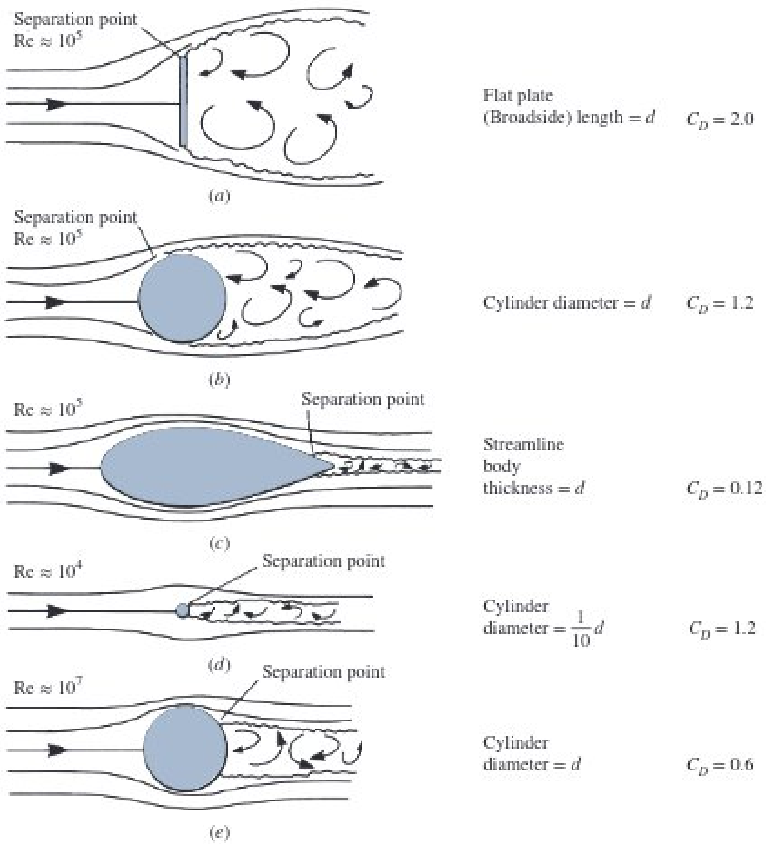

Figure 1.54 Drag coefficients for various aerodynamic shapes. (*Source:* Talay, T. A., *Introduction to the Aerodynamics of Flight,* NASA SP-367, 1975.)

Figure 25: Drag Coefficient

In Figure 25, provides various aerodynamic shapes, and based upon the Reynold's number the Drag coefficient can be approximated. In the table below, the final calculations which will be presented in the python code presented in order to simulate wind condition at various wind speeds and direction. Some of these values such as Reynold's number and drag coefficient will change.

Table 23: Oscillation Calculation Results

Results from Calculations		
Reynold's Number	Re	55227.695 (Assumed V=20ft/s)
Drag Coefficient	Cd	1.2
Drag Force	Fd	0.262 lbf
Stiffness	k	3257002 lb/ft
Natural frequency	Omega(0)	15.4
Damping Ratio	Zeta	0.128

In figure 26, a 3-Dimensional free body diagram for the load acting on the refinery stack and the support system is shown. The wind load will be strictly horizontal, and the drag force will be in that same line of action when hitting the structure.

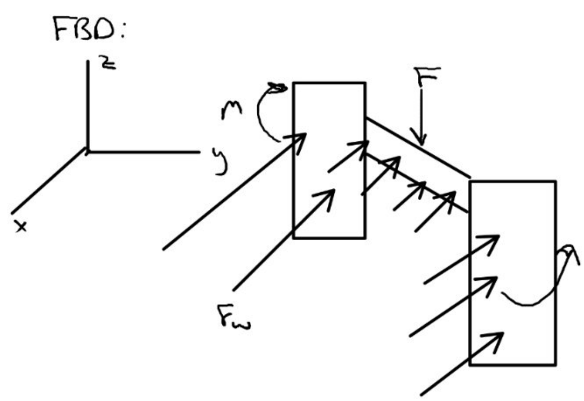

Figure 26: Free-Body Diagram

Similarly to Figure 25, Figure 27 shows the wind direction from west to east, or traversing horizontally. The oscillation of the stacks transitions from the y-axis to the x-axis.

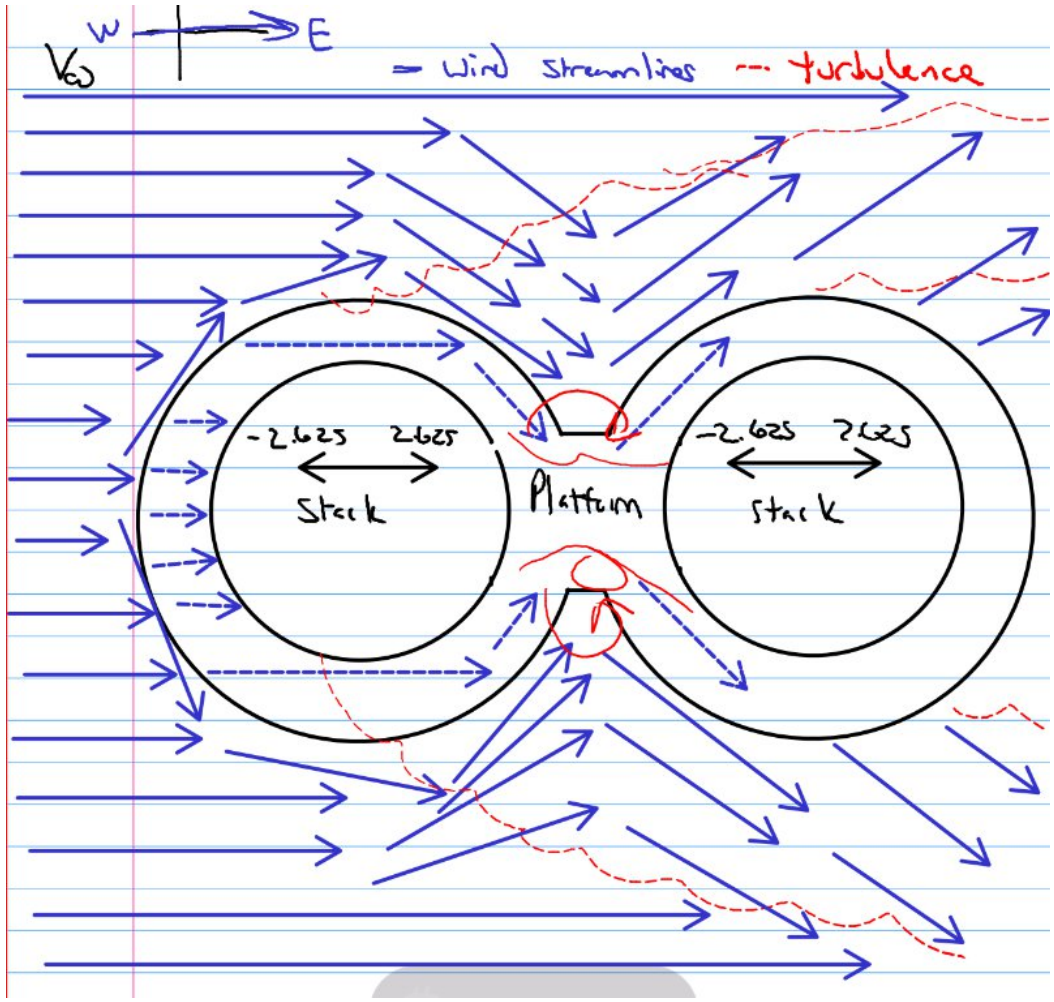

Figure 27: Velocity streamlines going West to East

In figure 28, the approximation of the flow transition from laminar flow to turbulent flow as the flow is going around the refinery stack and the platform.

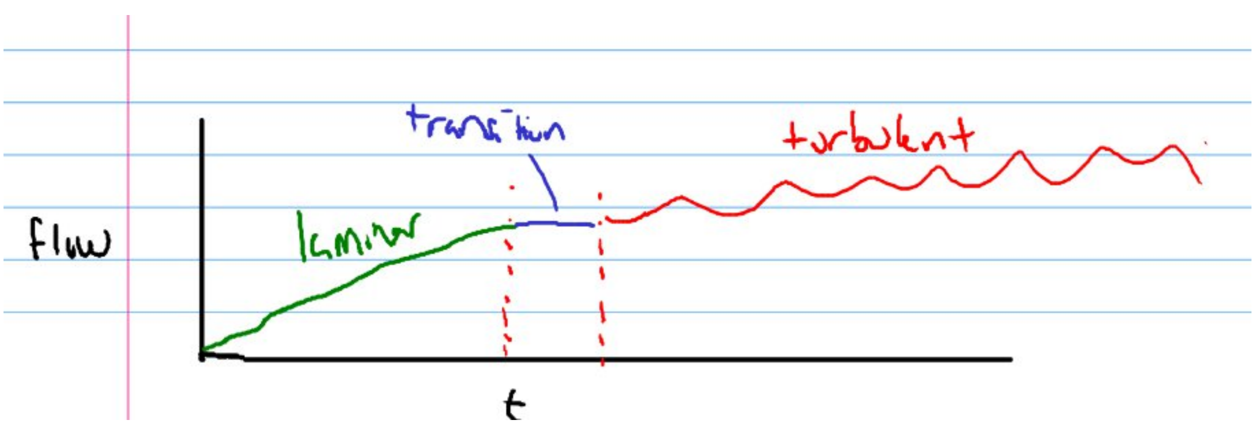

Figure 28: Flow from Laminar to Turbulent

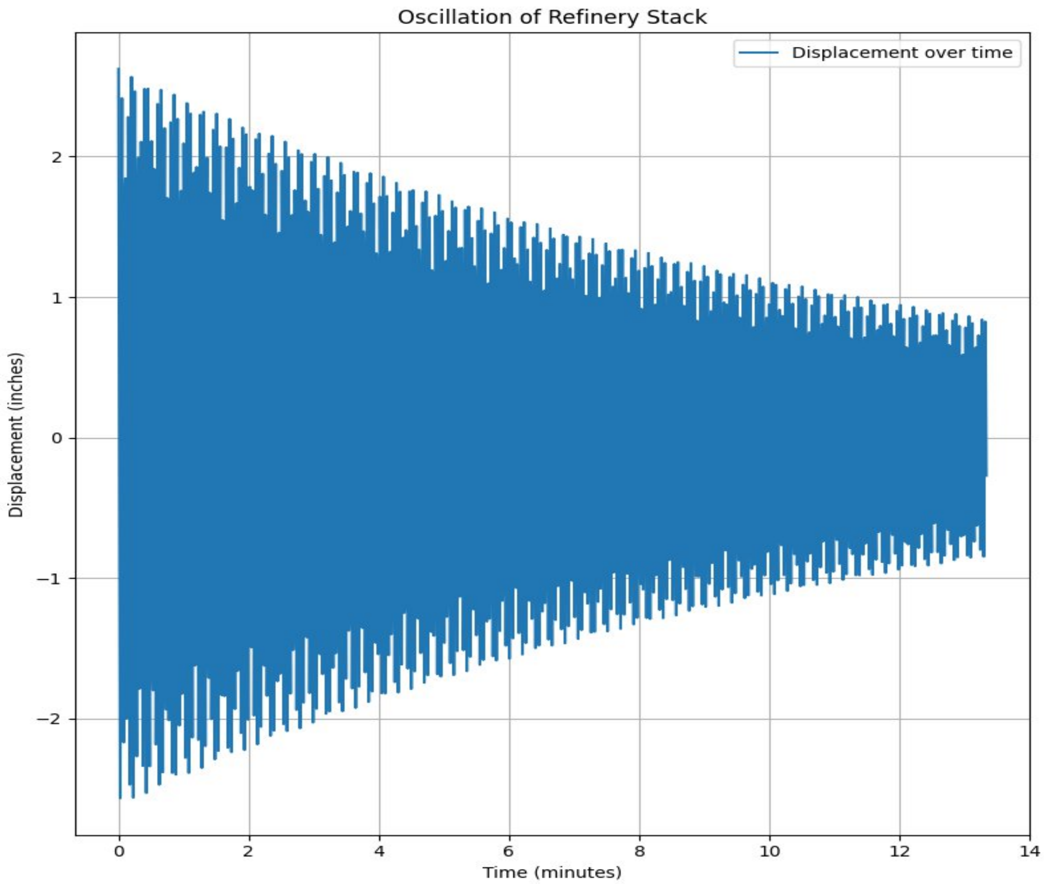

Figure 29: Oscillations of Refinery Stack

Figure 29 above shows the oscillation of refinery stack when the dampening coefficient is zero. Therefore, the current model does not have any damping, so it would not complete the time constraint to complete one period.

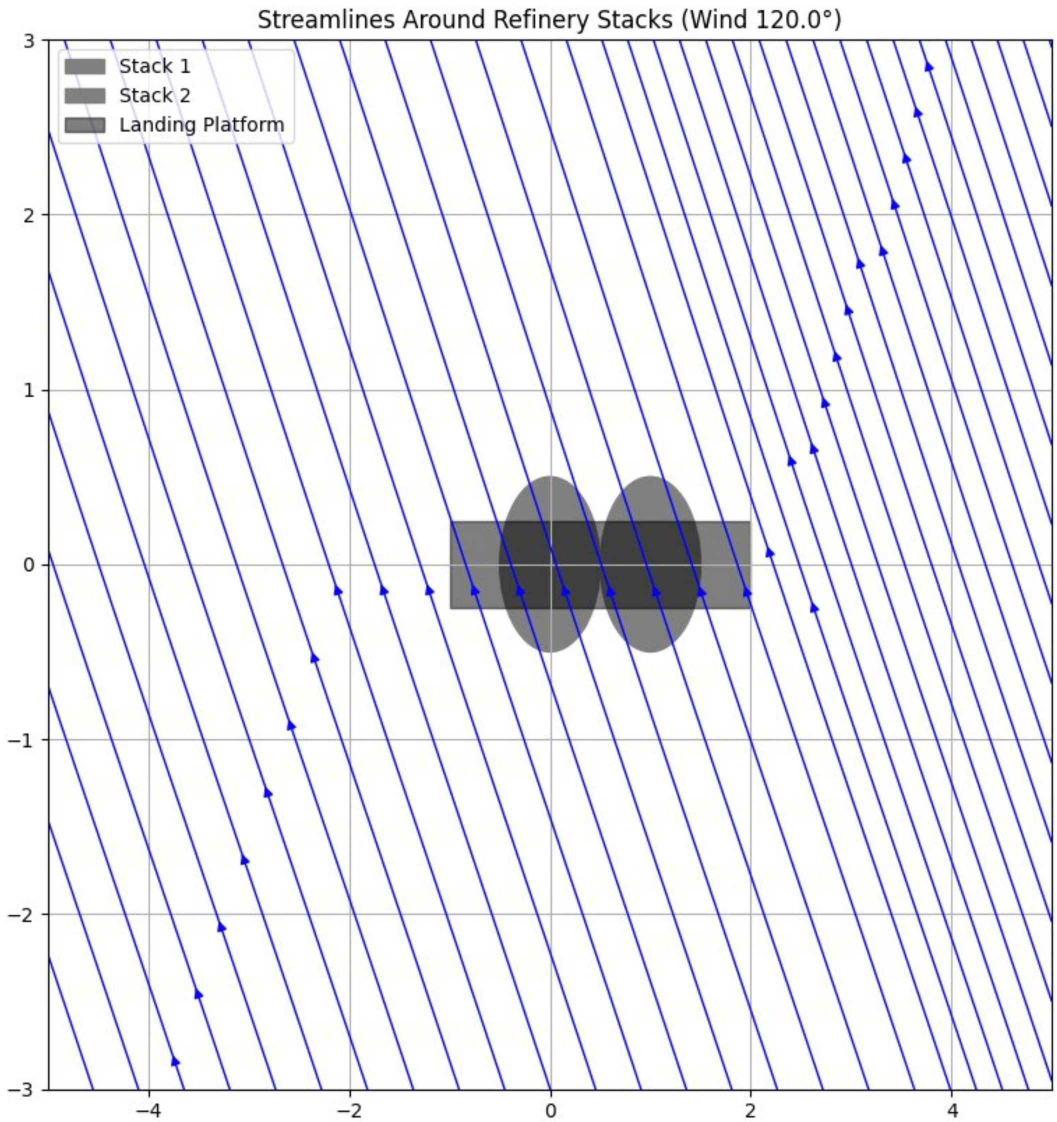

Figure 30: Results from Python Code Velocity streamlines at 120 degrees

This plot above in Figure 30 is from the code provided in the appendix. The objective of the code is to find the damping of the entire system of the refinery stack. Figure 30 has velocity vector streamlines where the wind is travelling at 120 degrees. The python code core objective is to simulate the reaction of the wind load at various velocity rates and at different directions to see how the refinery stack will react to the different wind speeds and directions. As of now, the code is still incomplete, and the goal is to complete it by the final submission.

Optimization

The following table outlines the analytical results from an extensive evaluation of multiple standard beam configurations, specifically designed to identify the most suitable dimensions for our application. This comprehensive analysis ensures that our design team did not arbitrarily select beam dimensions, but rather systematically optimized them based on critical performance metrics and economic considerations.

Table 24: Analytical results comparing beam configurations based on structural performance and cost efficiency.

Beam Dimensions					Weight	Vertical Bending Stress	Vertical Deflection	Horizontal Bending Stress	Horizontal Deflection	Factor of Safety	Vertical Stress W/ FoS	Pass	Fail	Actual FoS - Vertical	Horizontal Stress W/ FoS	Yield Stress of Material	Allowable Stress	Pass	Fail	Actual FoS - Horizontal	Cost			Results
Base (in)	Height (in)	Flange Thk (in)	Web Thk (in)	CSA (in^2)	(lb)	(psi)	(in)	(psi)	(in)	(-)	(psi)				(psi)	(psi)	(psi)				per lb $	per ft $	Total $/10ft	
6.02	6.20	0.260	0.260	4.610	139	1986	-7.81E-03	4688	-2.01E-02	3	5958			6.09	14064	36259	12086			2.58	2.75	38.25	382.50	FAIL
6.08	6.38	0.320	0.320	5.728	172	1583	-6.05E-03	3733	-1.59E-02	3	4750			7.63	11198	36259	12086			3.24	2.78	47.85	478.50	PASS
6.50	7.93	0.245	0.245	5.005	152	1449	-4.46E-03	4274	-1.70E-02	3	4347			8.34	12822	36259	12086			2.83	3.02	45.90	459.00	FAIL
6.54	8.06	0.285	0.285	5.862	178	1230	-5.88E-05	3623	-1.43E-02	3	3690			9.83	10869	36259	12086			3.34	3.19	56.70	567.00	PASS
8.00	8.00	0.285	0.285	6.678	203	1043	-3.18E-03	2422	-7.82E-03	3	3130			11.58	7267	36259	12086			4.99	2.92	59.28	592.80	PASS
8.02	10.10	0.350	0.350	8.904	269	648	-1.57E-03	1962	-6.32E-03	3	1945			18.64	5885	36259	12086			6.16	3.20	86.00	860.00	PASS

Table 22 shows the optimal beam dimensions identified through our evaluation are 6.08 inches (base) by 6.38 inches (height), with flange and web thicknesses of 0.32 inches. This beam configuration demonstrated superior performance in critical categories. Specifically, the vertical and horizontal stresses with applied factors of safety (FoS) were 4750 psi and 11198 psi, respectively, well below the allowable stress of 12086 psi. Furthermore, the vertical deflection at 6.05E-03 inches and horizontal deflection at 1.59E-02 inches were minimal, affirming structural integrity under load conditions. Notably, the actual achieved vertical factor of safety was 7.63, significantly surpassing our initial goal of 3, and the actual horizontal factor of safety was 3.24, also exceeding our target, thereby ensuring enhanced safety and reliability.

Economic efficiency was a vital component of our decision-making process, as reflected in the cost analysis section of the table. The selected beam configuration presents a highly favorable cost profile at $2.78 per pound and $47.85 per foot, culminating in a total cost of $478.50 per 10 feet. Balancing structural requirements and economic feasibility ensures that resources are used efficiently, without compromising safety or performance standards. Such diligence in cost consideration not only optimizes project budgets but also aligns with sustainable and responsible engineering practices.

The following bolt optimization table provides a comparative assessment of bolt diameters and materials under a constant applied load. The objective was to ensure that bolts could sustain the critical shear load without exceeding allowable shear stress limits, while also optimizing for a factor of safety of at least 3. This type of evaluation is crucial in mechanical design where fasteners must maintain structural integrity under operational stresses.

Table 25: Bolt optimization based on shear stress and safety factors across varying diameters.

Bolt Optimization

Material	Yield Stress	Diameter	CSA	Critical Load	Critical Shear Stress	Allowable Shear Stress	Factor of Safety
	psi	in	in^2	lbf	psi	psi	n >= 3
Medium	92000	0.25	0.05	1239	25241	53084	2.10
Carbon	92000	0.3125	0.08	1239	16154	53084	3.29
Steel	92000	0.375	0.11	1239	11218	53084	4.73
	92000	0.5	0.20	1239	6310	53084	8.41

Table 23 evaluates four bolt configurations using a constant critical load of 1239 lbf. As the diameter and cross-sectional area (CSA) of the bolts increase, the critical shear stress decreases significantly, reducing the risk of material failure. For example, a 0.25-inch diameter bolt produced a critical shear stress of 25,240 psi, resulting in a low factor of safety of 2.10—below the acceptable threshold. In contrast, a 0.3125-inch diameter bolt reduced the critical shear stress to 16,154.05 psi and achieved a factor of safety of 3.29, just above the target. The safest and most efficient option was the 0.5-inch diameter bolt, which resulted in a shear stress of only 6310 psi and a factor of safety of 8.41. These results underscore the importance of bolt size in load-bearing applications and reinforce the principle that careful material and geometry selection can greatly enhance both safety and performance.

See excel file for more calculation details and more analytical results.

Calculations (3).xlsx

Failure Theory and Fatigue Analysis

Failure theory is essential for predicting when and how a structural component may fail under various loading conditions. In this project, which involves designing a support beam system for refinery stacks, several stresses were evaluated to ensure the design could withstand wind, temperature shifts, and oscillatory stack movement (2.625 inches every 13 minutes). Basic stress equations were used throughout the analysis, such as normal stress:

Equation 40: Stress

$$\sigma = \frac{F}{A}$$

and bending stress:

Equation 41: Bending Stress

$$\sigma = \frac{Mc}{I}$$

where F is the applied force, A is the cross-sectional area, M is the bending moment, c is the distance from the neutral axis, and I is the moment of inertia.

Additionally, deflection was checked using:

Equation 42: Maximum Deflection

$$\delta_{max} = -\frac{wl^4}{384EI}$$

to confirm minimal displacement under live loads and wind. Calculations showed a maximum deflection of only 0.00149 inches under ideal conditions and 0.00523 inches under worst-case wind loads, indicating excellent stiffness and structural performance.

Since the beam and its fasteners are exposed to cyclic loading, fatigue failure was a major concern. The Goodman fatigue criterion is applied to evaluate long-term durability under alternating and mean stress:

Equation 43: Goodman Fatigue

$$\frac{\sigma_a}{S_e} + \frac{\sigma_m}{S_{ut}} = \frac{1}{n}$$

where $\sigma_a = \frac{\sigma_{max} - \sigma_{min}}{2}$ is the alternating stress, $\sigma_m = \frac{\sigma_{max} + \sigma_{min}}{2}$ is the mean stress, S_e is the endurance limit, S_{ut} is the ultimate tensile strength, and n is the factor of safety.

For bolts subjected to worst-case shear, the calculated shear stress was:

Equation 44: Shear Stress

$$\tau = \frac{F}{A} = \frac{1239 lbf}{1.767 in^2} = 701.19 \; psi$$

The safety factor in shear using von Mises criterion was then:

Equation 45 Factor of Safety

$$n_d = \frac{0.577 * \; S_y}{\tau} = \frac{0.577 * \; 92000}{701.19} \approx 75$$

which reflects very conservative, safe design under repeated load cycles. Welds were also analyzed for strength, requiring only a 0.024-inch throat to safely support 1,958 lbf.

Overall, the application of failure theory—especially Goodman fatigue analysis and von Mises stress criteria—informed each major design choice, from beam sizing to weld and bolt specification. The use of slotted holes and flexible connections accounted for thermal expansion and stack oscillations, while dual I-beams improved load distribution. These measures, supported by both analytical equations and FEA validation, produced a support system capable of withstanding high-cycle fatigue, harsh environmental conditions, and dynamic loading. The result is a robust, refinery-ready structural solution with a long service life and high reliability.

Incorporate the life of the design/beam. How many years will it last?

CAD Drawings

Computer-Aided Design (CAD) drawings not only provide a visualization of the design plan, but also aid in understanding the parameters, dimensions, and assembly of the design. The technical illustrations below create a visual reference of the beam design, fitted according to the specified constraints and requirements. Including CAD drawings in this report allows for effective collaboration among design team members, facilitates accurate manufacturing, and communicates to the reader the vision for the design. They serve as the bridge between theoretical calculations and practical implementation, making them an essential part of design documentation.

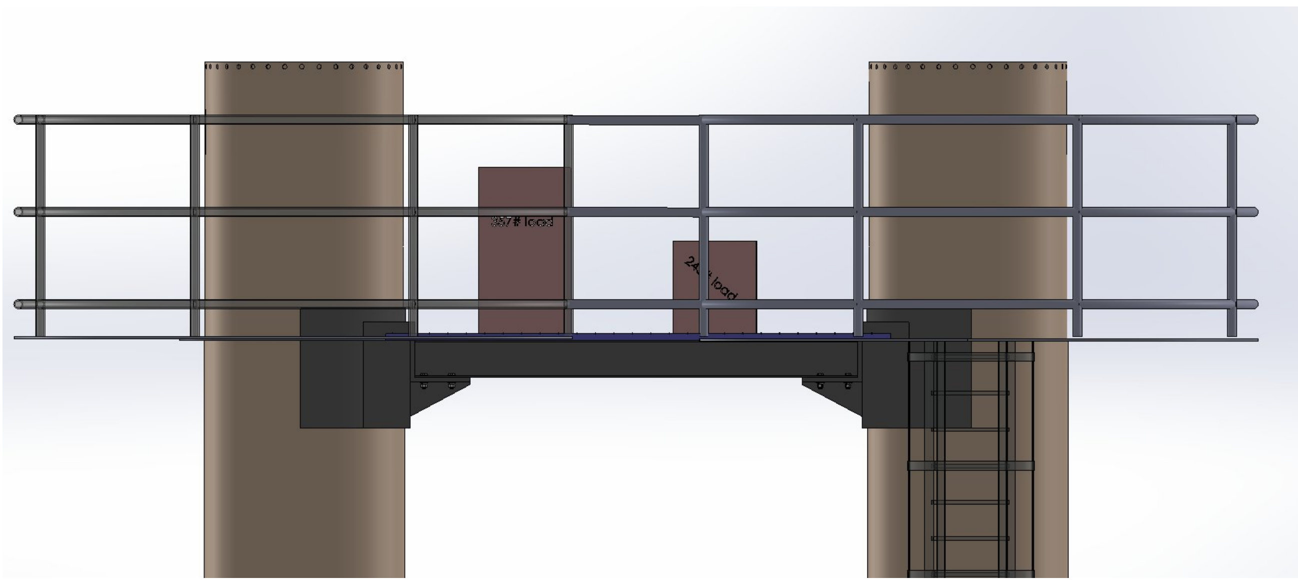

Figure 31: Right side view of refinery stack

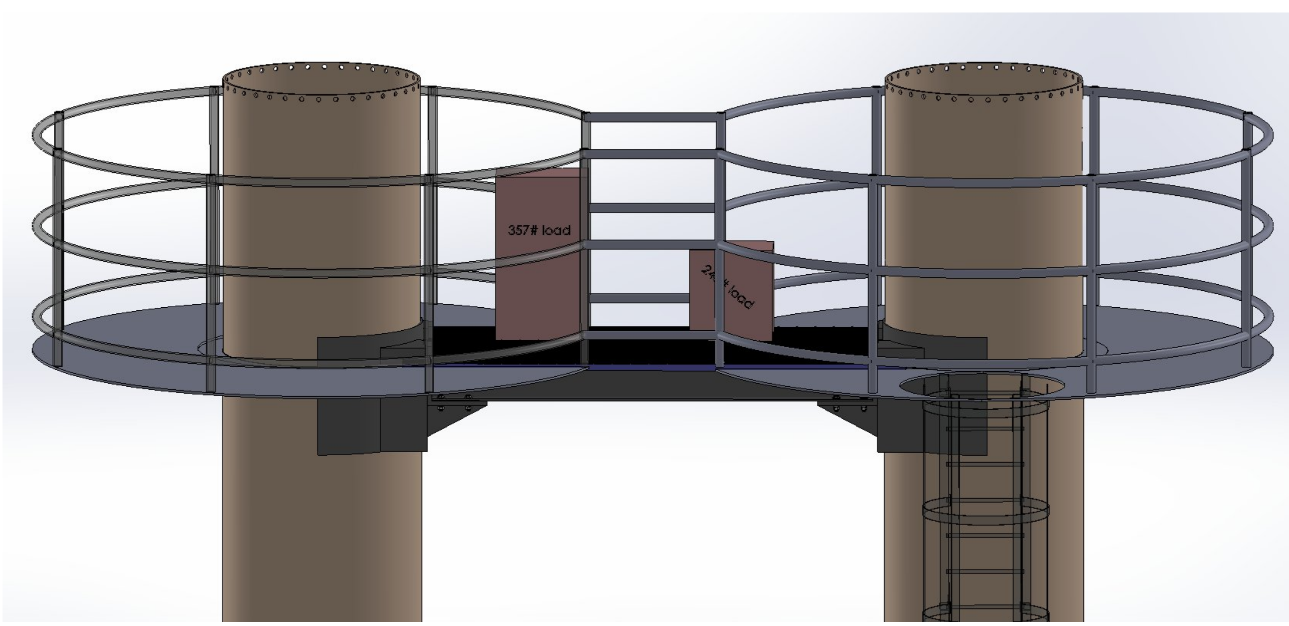

Figure 32: Left side view of refinery stack

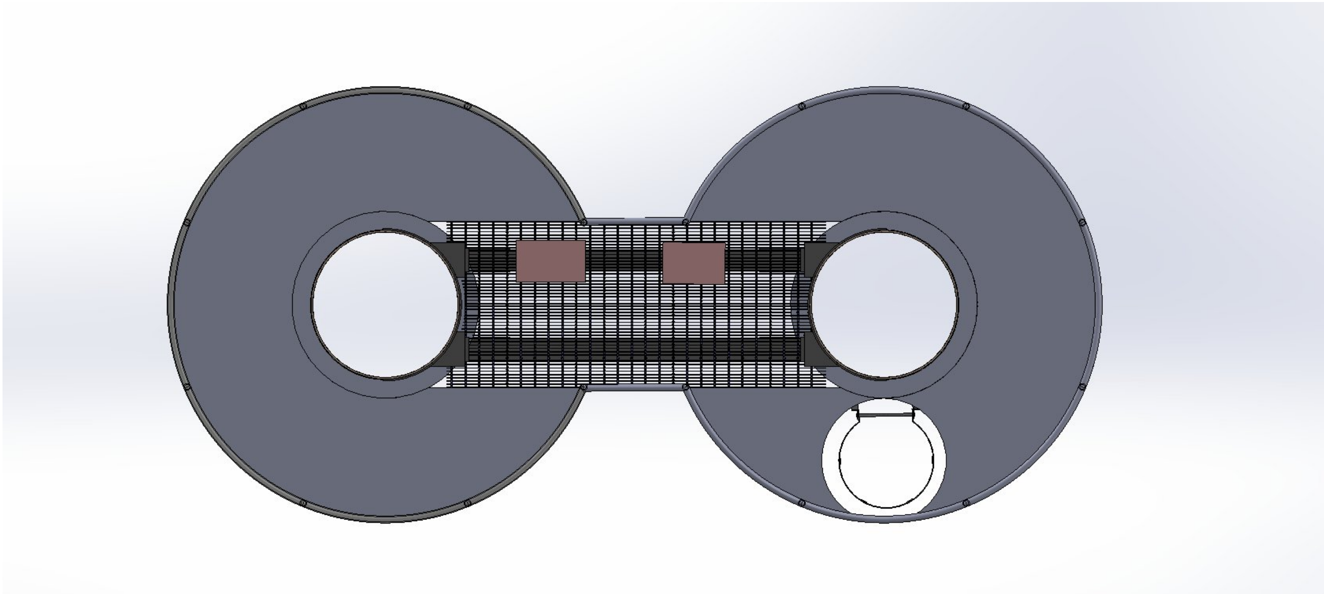

Figure 33: Top view of refinery stack

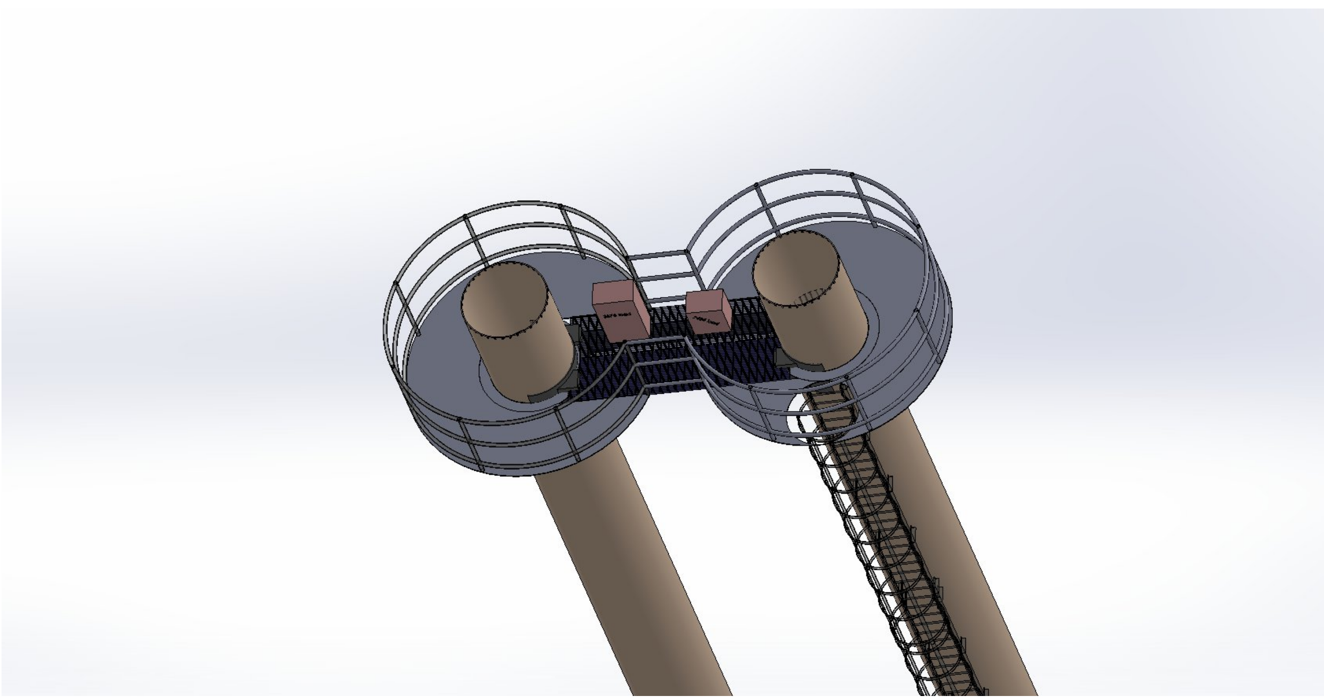

Figure 34: Top view of Overall Refinery stack with support system design

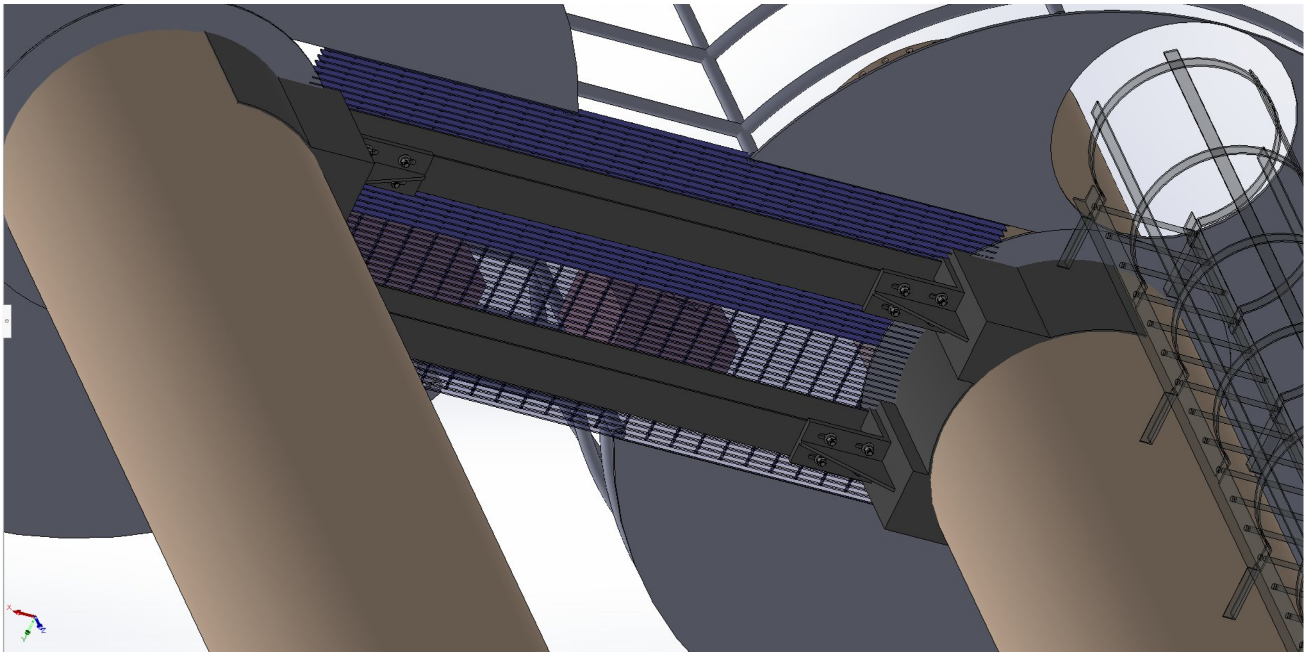

Figure 35: Bottom view overall support system

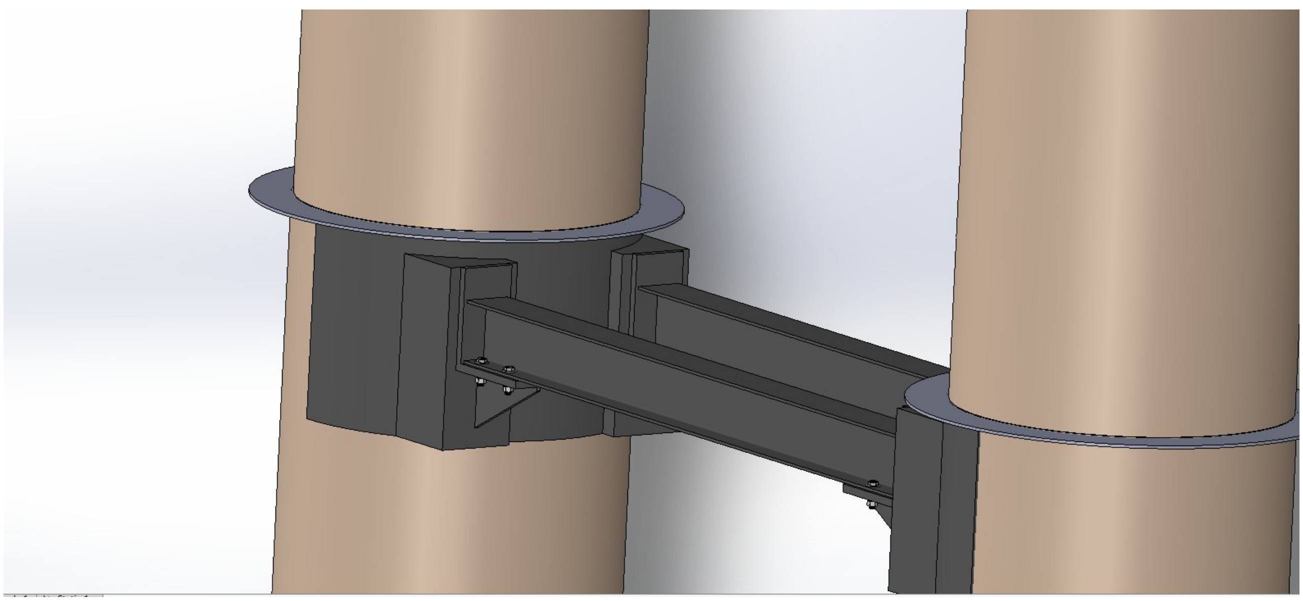

Figure 36: Side View of overall support system

Figures 37-39 below show the CAD drawings for the bolt connections.

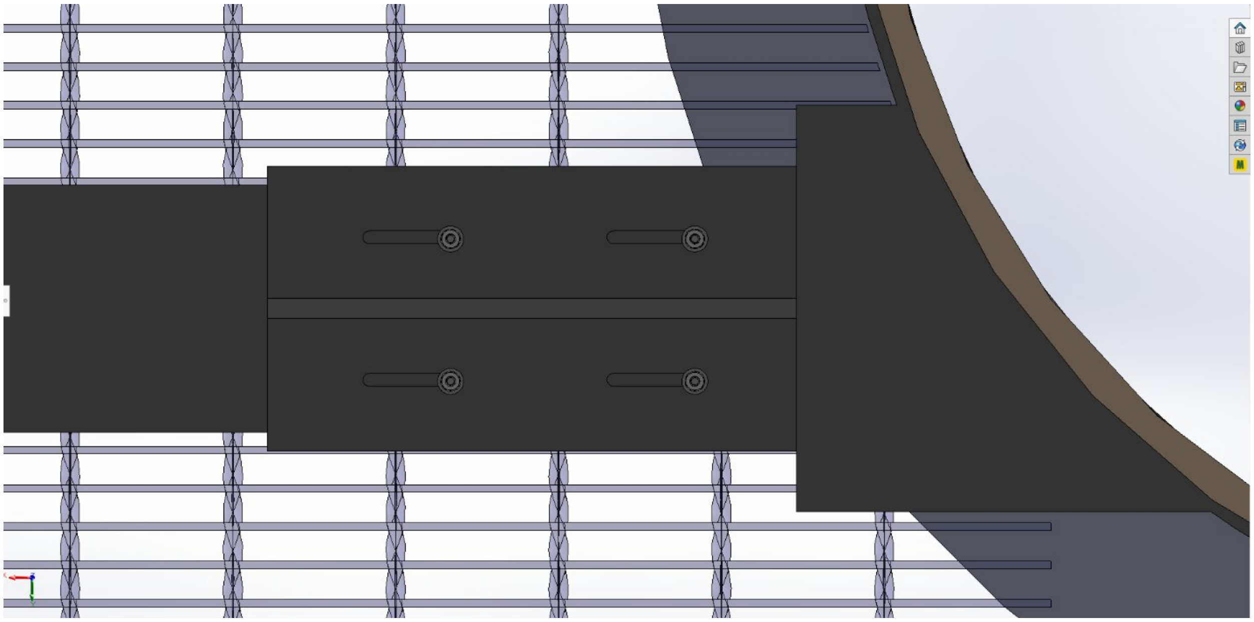

Figure 37: Bottom View Slotted Bolts and with Collar

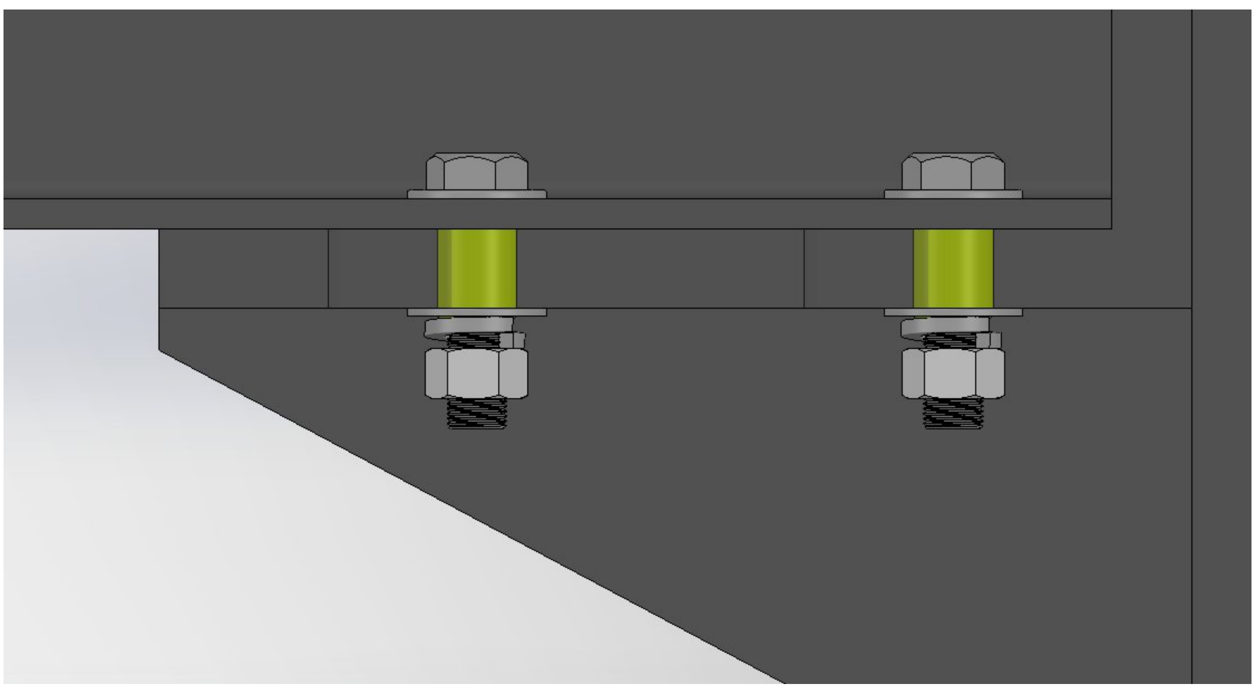

Figure 38: Side View Bolts positioning

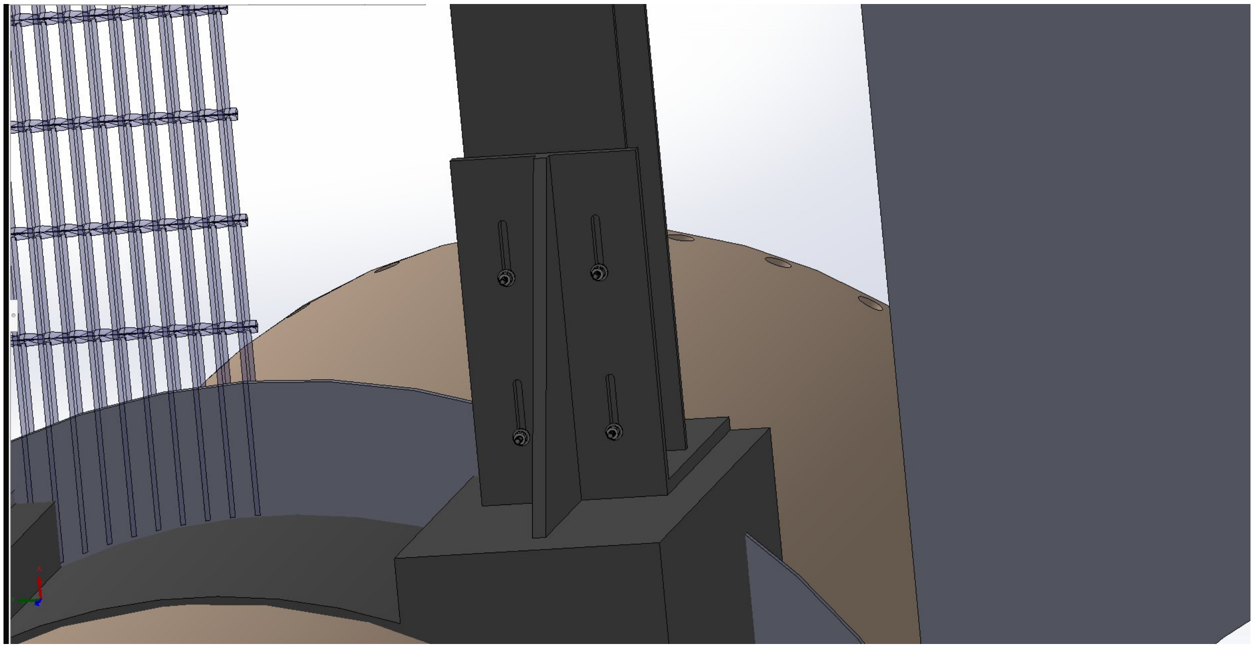

Figure 39: Bottom view of the Beam with support

FMEA

FMEA (Failure Modes and Effects Analysis) is a systematic method used to identify, evaluate, and prioritize potential failure modes within a system. It helps the team understand how different components or processes might fail and the impact these failures could have on the flare stack and surround structures. The goal is to proactively identify areas of risk, prioritize them, and implement strategies to mitigate or eliminate these risks. While it does not take the place of risk analysis, it is a helpful aid in managing these risks.

Function	Failure	Effect	Si	Cause	Oi	Control	Control Type	Di	RPN i	Recommended Action	Person Responsible	Planned Completion Date	Actual Completion Date	Sr	Or	Dr	RP Nr
Beam																	
Support grating, support flares	Excessive deflection	Structural damage, OSHA	9	Undersized I beam	7	Design calculations	Prevention	4	252	Redesign Beam Size	Clinton	3/15/2025	3/15/2025	9	1	1	9
						Simulations	Prevention										
Connections																	
Connect flares to beam	hardware backs out over time	Flares fall, catwalk falls	9	Missing lock washers	8	Oversight on design	Prevention	4	288	Add lock washers to design	Peter	3/15/2025	3/15/2025	9	3	2	54
Connect flares to bean	Hardware corrodes	Flares fall, catwalk falls	9	Steel hardware corrodes over time	8	Oversight on design	Prevention	4	288	Change hardware to stainless steel	Clinton	3/1/2015	3/1/2025	9	2	2	36
Grating																	
Support catwalk, equipment, personell	Grating bends	Gaps, equipment fall, personel safety at risk	7	Overloading the platform	2	Signage about maximum weight	Prevention	3	42								
						maintenance inspection	Detection										
Maintain integrity	Loss of integrity	breakage	7	incorrect materials selected for design	4	Verify necessary material	Prevention	2	56	Utilize stainless grating instead of galvanized	Peter	3/1/2015	3/10/2025	7	3	1	21
Flares																	
Burn off gases	Overburning, exceeding max temps	Loss of beam integrity	6	Overflaring	2	Safety shut down	Prevention	4	48								
	corrosion	Loss of grate integrity	7	Overflaring	2	Install temp probes on flare	Detection	3	42								

Figure 40: FMEA

FEA Analysis

The Finite Element Analysis (FEA) was conducted using SolidWorks Simulation to evaluate deflection of the support beam system under both ideal and worst-case loading conditions. The primary goal was to validate structural performance, compare with previously mentioned hand-calculated and online calculated values, and account for 3D effects such as shear deformation and torsion.

Simulation Setup:

- **Beam Length:** 97 inches
- **Material:** A36 Steel
- **Web Height:** 5.75 inches
- **Boundary Conditions:** Brackets fixed at both ends
- **Mesh Type:** Solid mesh with refinement near load and support locations

Case 1: Ideal Conditions

Finite Element Analysis was run based upon the optimized beam size and the appropriate loading as state previously. FEA is not used to determine the beam size or appropriate loading, its simply used to support and verify the calculations already made. The max deflection in ideal conditions would be 0.001305” at the center.

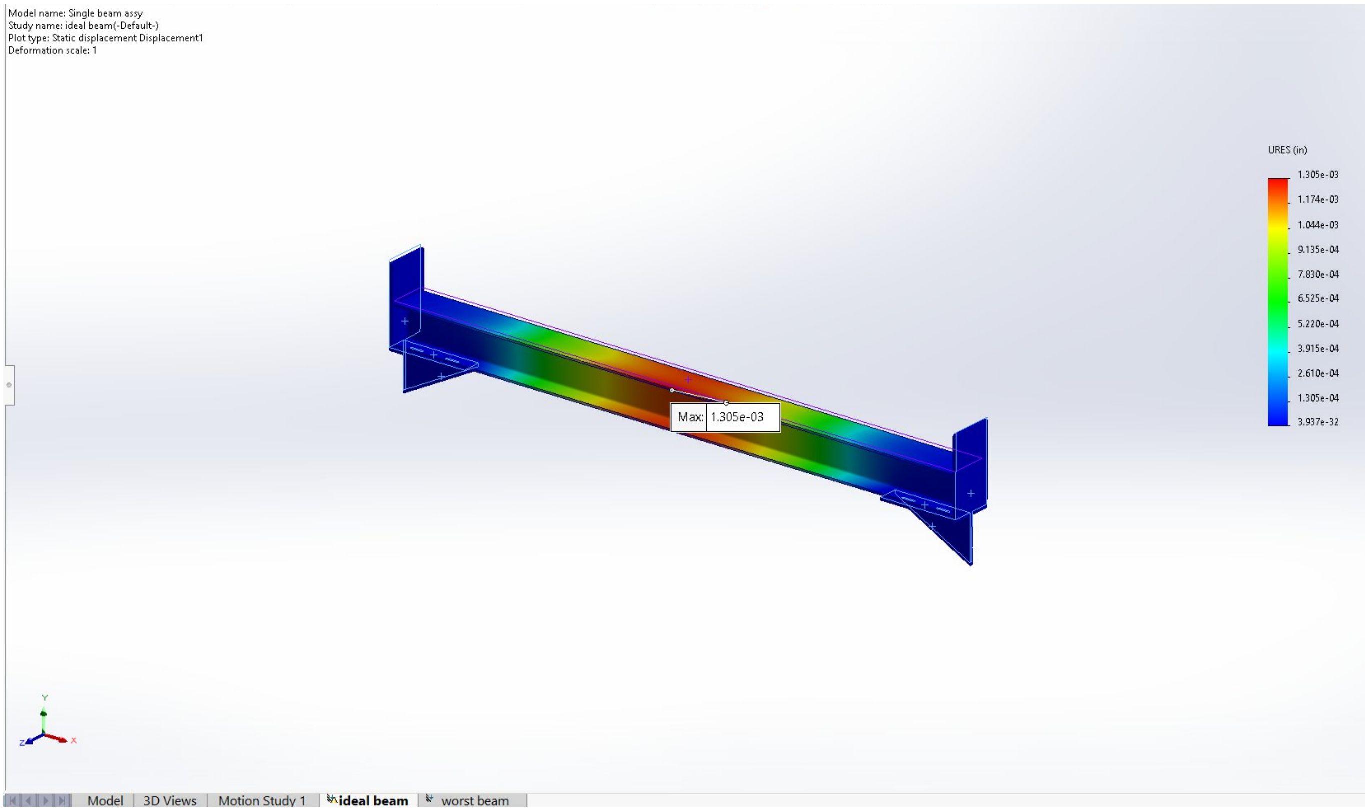

Figure 41: Ideal Conditions FEA

Case 2: Worst Conditions

FEA is not used to determine the beam size or appropriate loading in the worst case scenario, its simply used to support and verify the calculations already made. The max deflection in worst case conditions is 0.00819” at the center

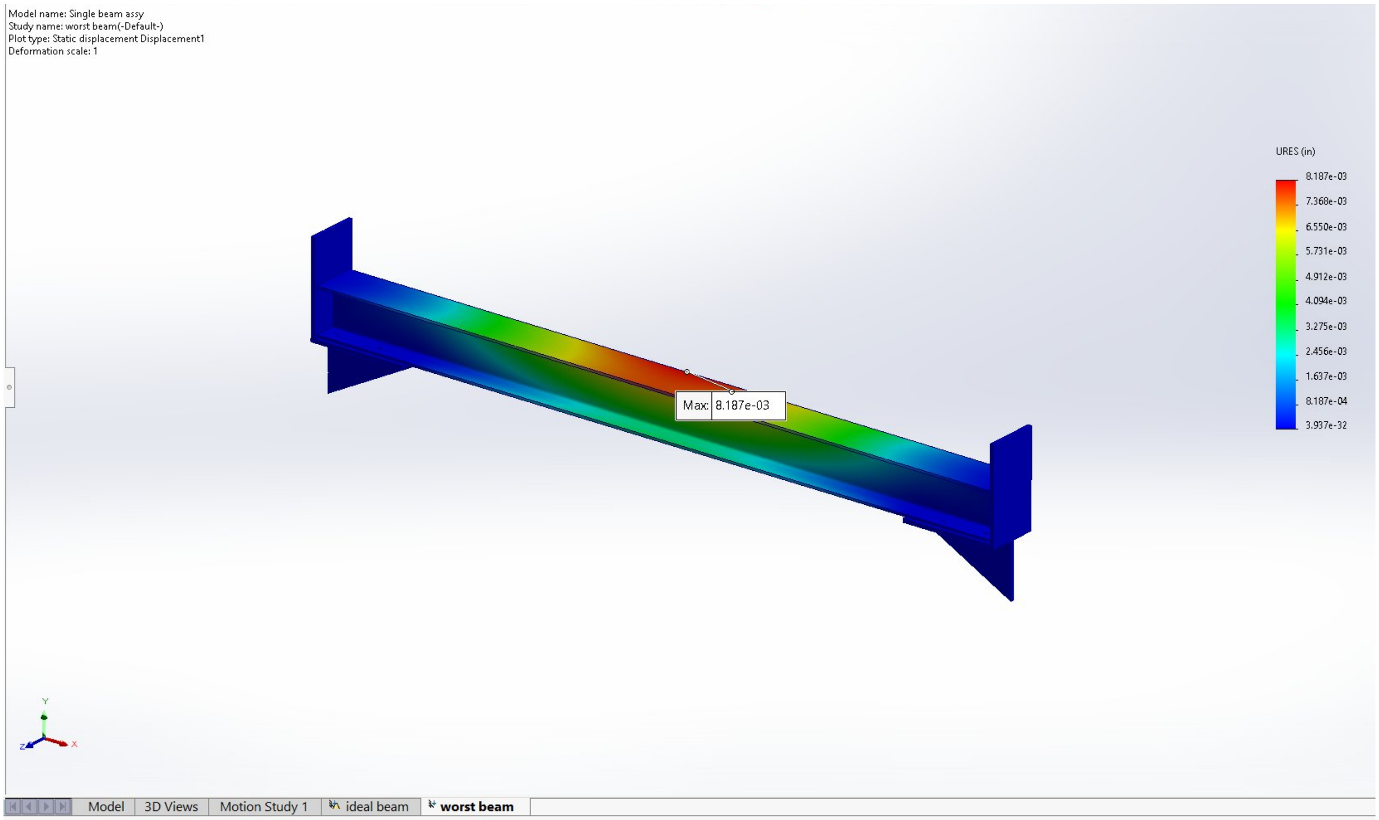

Figure 42: Worst Case FEA

A comparison of the calculated and simulated results includes the maximum deflection and the percent variation

Table 26: Deflection Comparison

Scenario	Hand-Calc Deflection (in)	FEA Deflection (in)
Ideal-Case Conditions (12% Variance)	0.00149	0.001305
Worst-Case Conditions (76% Variance)	0.00465	0.00819

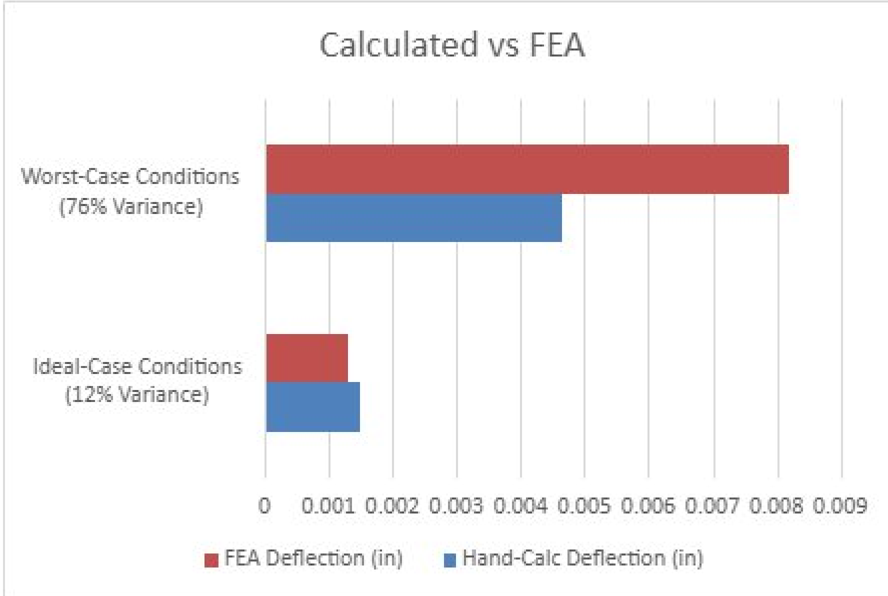

Figure 43: Calculated vs FEA comparison

The FEA-predicted maximum deflection under ideal case results closely match previously provided calculations, providing confidence in the model accuracy. Under worst-case lateral loading, the beam demonstrates acceptable flexibility and structural performance within expected safety margins.

The FEA-predicted maximum deflection under worst-case wind loading was **0.0082 in**, compared to a hand-calculated deflection of **0.0047 in** using beam theory. The difference is attributed to additional 3D effects such as torsion, shear deformation, and slight support flexibility that are not captured in 1D analytical models but are accurately resolved in the SolidWorks Simulation environment. A small variance is to be expected and not problematic to the overall solution. Another component to consider is that the simulated model was slightly more realistically fixtured to the subcomponents, as it would be seen in a real fabricated environment.

Conclusion

The design and analysis of the refinery stack support beam system represent a comprehensive application of mechanical design principles, structural analysis, and real-world engineering judgment. Through careful evaluation of operational demands such as live loads, wind pressures, thermal effects, and cyclic oscillations, the team developed a solution that not only meets but exceeds the performance requirements for a dynamic refinery environment.

The dual I-beam configuration was selected to optimize load distribution, enhance system redundancy, and simplify transportation and field assembly. Connection strategies, including bolted joints, fillet welds, slotted holes, and spacers, were deliberately chosen to accommodate stack movement, minimize stress concentrations, and extend the system's fatigue life. Material selections, weld sizing, bolt optimization, and structural dimensions were validated through detailed hand calculations, online simulations, and SolidWorks FEA, ensuring that all components maintain conservative safety margins well above critical thresholds.

Failure modes and fatigue risks were systematically evaluated using established theories such as the Goodman fatigue criterion and von Mises yield analysis. The design achieves safety factors of over 3 for welded joints and bolted connections and demonstrates minimal deflection under both ideal and worst-case loading conditions. These results confirm that the structure will maintain its integrity over a long service life, estimated at over 20 years under expected refinery operating conditions.

Ultimately, this project demonstrates a successful integration of theoretical knowledge, industry standards such as ASME STS-1, and practical design considerations. The final support system balances strength, flexibility, durability, and maintainability, ensuring reliable performance even under the harshest environmental conditions. The design not only addresses the immediate structural needs but also incorporates long-term reliability and ease of inspection, repair, and modification, offering a robust and forward-thinking solution.

References

Abakus, A. (2019, September 27). *Wind effect on piping systems*. Piping Stress. Retrieved from https://www.pipingstress.net/piping-stress-support-engineering/wind-effect-on-piping

Budynas, R. G., & Nisbett, J. K. (2019). *Shigley's mechanical engineering design* (11th ed.). McGraw-Hill Education.

Tatools Online. (n.d.). *Safety data: Bolt strengths identification*. Retrieved from http://www.tatoolsonline.com/uploads/266/safety_data_bolt_strengths_identification.pdf

Material Properties. (n.d.). Retrieved from https://material-properties.org/

Concawe Risk Assessment Ad-hoc Group. (1982). *Methodologies for hazard analysis and risk assessment in the petroleum refining and storage industry* (Report No. 10/82). Concawe. Retrieved from https://www.concawe.eu/wp-content/uploads/2017/01/rpt_82-10ocr-2004-01738-01-e.pdf

Palm, W. J., III. (2021). *System dynamics* (4th ed.). McGraw-Hill. https://www.mheducation.com/highered/product/system-dynamics-palm/

Anderson, J. D., Jr. (2024). *Fundamentals of aerodynamics* (7th ed.). McGraw-Hill. https://www.mheducation.com/highered/product/fundamentals-aerodynamics-anderson/

American Society of Mechanical Engineers. (2000). *ASME STS-1-2000: Steel stacks*. American Society of Mechanical Engineers.

National Institute of Standards and Technology. (2005). *Effects of non-uniform high heat exposure on steel I-beams* [PDF]. National Institute of Standards and Technology. Retrieved from https://tsapps.nist.gov/publication/get_pdf.cfm?pub_id=912962

Seshadri, R., Buell, J., & Mehta, A. (2005). Structural response of flare stacks to induced oscillations. *Journal of Wind Engineering and Industrial Aerodynamics, 93*(5), 371–386. https://doi.org/10.1016/j.jweia.2005.02.001

https://www.engineeringtoolbox.com/air-absolute-kinematic-viscosity-d_601.html

Appendix

Oscillation Python Code

```
import numpy as np
import matplotlib.pyplot as plt
import matplotlib.animation as animation
from scipy.integrate import solve_ivp

# Convert constants to English units
ft_to_in = 12
slug_to_lb = 32.174

# Given parameters from calculations
m = (1663.63 + 1040.88) / slug_to_lb  # Convert force (lbf) to mass (slugs)
k = 1.85e7 / ft_to_in  # Convert stiffness from lbf/ft to lbf/in
c = float(input("Enter damping coefficient (lbf·s/in, enter 0 if negligible): "))
v = float(input("Enter wind speed (ft/s): "))
C_d = 1.2  # Drag coefficient (assumed)
A = 18  # Cross-sectional area in in²
rho = 0.002377  # Air density in slugs/ft³
F_wind = 0.5 * C_d * A * rho * (v**2)  # Wind force (lbf)
L = 109.5  # Beam length in inches
I = (1/12) * 6 * (8**3)  # Moment of inertia for I-Beam in in^4

# Calculating natural and damped frequencies
omega_n = np.sqrt(k / m)  # Natural frequency (rad/s)
zeta = c / (2 * np.sqrt(m * k))  # Damping ratio
omega_d = omega_n * np.sqrt(1 - zeta**2) if zeta < 1 else 0  # Damped frequency

# Time settings
time = np.linspace(0, 800, 1000)  # Time array (seconds)
A_disp = 2.625  # Amplitude in inches

# Define differential equation
def system(t, y):
    x, v = y
    M_wind = F_wind * L  # Wind-induced moment
    dxdt = v
    dvdt = (-c * v - k * x + M_wind / I) / m
    return [dxdt, dvdt]

# Solve using solve_ivp
y0 = [A_disp, 0]
sol = solve_ivp(system, [0, max(time)], y0, t_eval=time, method='RK45')

# Extract displacement
disp = sol.y[0]
```

```
# Plot results
plt.figure(figsize=(10, 6))
plt.plot(time / 60, disp, label="Displacement over time")
plt.xlabel("Time (minutes)")
plt.ylabel("Displacement (inches)")
plt.title("Oscillation of Refinery Stack")
plt.legend()
plt.grid()
plt.show(block=True)

# Streamline plot with user-input wind direction
angle_deg = float(input("Enter wind direction in degrees (0 to 360, step of 15): "))
angle_rad = np.radians(angle_deg)

x = np.linspace(-5, 5, 100)
y = np.linspace(-5, 5, 100)
X, Y = np.meshgrid(x, y)
U = v * np.cos(angle_rad) + 0.2 * np.sin(Y)  # Wind profile along the input direction
V = v * np.sin(angle_rad) + 0.1 * np.cos(X)

fig2, ax2 = plt.subplots(figsize=(8, 6))
ax2.streamplot(X, Y, U, V, density=1.5, color='b', linewidth=1)
ax2.add_patch(plt.Circle((0, 0), 0.5, color='gray', label="Stack 1"))
ax2.add_patch(plt.Circle((1, 0), 0.5, color='gray', label="Stack 2"))
ax2.add_patch(plt.Rectangle((-1, -0.25), 3, 0.5, color='black', alpha=0.5, label="Landing Platform"))
ax2.set_xlim([-5, 5])
ax2.set_ylim([-3, 3])
ax2.set_xlabel("")
ax2.set_ylabel("")
ax2.set_title(f"Streamlines Around Refinery Stacks (Wind {angle_deg}°)")
ax2.legend()
plt.grid()
plt.show(block=True)
```